Chemical weathering of mafic rocks in boreal subarctic environment (northwest Russia) under influence of glacial moraine deposits

Ekaterina V. Vasyukova, Priscia Oliva, Jerome Viers, Francois Martin, Bernard Dupré, Oleg S. Pokrovsky

Chemical weathering of mafic rocks in boreal subarctic environment (northwest Russia) under influence of glacial moraine deposits

Ekaterina V. Vasyukova[1#], Priscia Oliva[1], Jerome Viers[1], Francois Martin[1], Bernard Dupré[1], Oleg S. Pokrovsky[1,2,3]*

[1]*Geoscience and Environment Toulouse (GET, UMR 5563), University of Toulouse, OMP-CNRS; 14, avenue Edouard Belin, 31400 Toulouse, France*

[2] *N. Laverov Federal Center for Integrated Arctic Research, Russian Academy of Science, Nab. Severnoy Dviny 23, 163000 Arkhangelsk, Russia,*

[3] *BIO-GEO-CLIM Laboratory, Tomsk State University, 36 Lenina, 634050 Tomsk, Russia*

* *Corresponding author email:* ***oleg.pokrovsky@get.omp.eu***

[#] *present address: WTE Wassertechnik GmbH, Ruhrallee 185, 45136 Essen, Germany*

Keywords: chemical weathering, mafic rocks, soil, fresh waters, boreal zone.

Submitted to *Chemical Geology*, after revision, 24 December 2018

Abstract

Chemical weathering of mafic rocks represents substantial sink of atmospheric CO_2 yet the mechanismes of this process in high-latitude regions are poorly understood. This work addresses geochemical migration and partitioning of major and trace elements between rock, soil and surface waters during chemical weathering of mafic rocks and soil formation under the influence of a glacial moraine in the northwestern Russian subarctic. We used multidisciplinary approach which included major and trace element chemical analysis, Sr isotopic measurements, and mineralogical structural and microscopic investigations. Quaternary (Pleistocene) deposits were observed even in the deepest horizons of soil profiles and confirm a strong moraine influence as most soils showed podzolic features. Chemical and Sr isotopic analyses revealed a strong impact of the moraine on soil chemistry and mineralogy. Mineralogical studies showed the presence of non-aeolian quartz and zircon in soils which were not linked to the nature of the parental rocks (i. e. mafic and felsic). At the same time, we observed the presence of etch pit corrosion on the surface of zircons and feldspars, and a newly-formed matter adjacent to the surface of primary phases. The chemical index of alteration (CIA) showed weak or no weathering of rocks within the soil profile and the weathering intensity scale confirmed the “felsic” chemical composition of soils developed over mafic and ultramafic rocks. Analysis of Sr radiogenic isotopes demonstrated preferential removal of easily weatherable and less radiogenic minerals over the full depth of soil profile and a more radiogenic signature of the granitic moraine compared to mafic and felsic bedrocks. The composition of most surface waters reflected the weathering of silicate rocks but did not allow for distinguishing purely mafic source. The chemical weathering rates of ultramafic rocks were calculated to be higher than those for the granitic till, but the moraine depositions which dominate this region hide evidence of the real weathering process. This could be due to retention of Mg and Ca in soil due to precipitation of secondary phases such

as Mg-vermiculite or divalent cation adsorption on mineral, organic or organo-mineral phases. As a result, weathering rates estimated for the olivinite rock appear to be lower than the weathering rates of mafic rocks reported in other boreal and subarctic regions. Overall, the felsic moraine deposits are capable to sizably decrease the weathering intensity of mafic rocks which should be taken into account for chemical weathering modelling of high-latitude regions subjected to glaciation in the past.

1. Introduction

Numerous works have emphasized the significant role of silicate weathering in atmospheric CO_2 consumption and climate regulation; it is considered to be the principal process for removing carbon dioxide from the atmosphere on a long-term scale (Berner et al., 1992, 1995; Boeglin and Probst, 1998; Berner and Caldeira, 1999; Gaillardet et al., 1999; Kump et al., 2000; Dupré et al., 2003). Weathering of continental basalts, accounting for about 30 % of total CO_2 consumption by silicate weathering (Dessert et al., 2003), has been extensively addressed (Gislason et al., 1996; Louvat and Allègre, 1997, 1998; Dessert et al., 2001; Grard et al., 2005; Pokrovsky et al., 2005, Schopka et al., 2011; Gaillardet et al.; 2011, Schoppa and Derry, 2012; Eiriksdottir et al., 2013, 2015; Balagizi et al., 2015; Dessert et al, 2015; Ibarra et al., 2016). Recently, it has been shown that the weathering of silicate and carbonate rocks in the Baltic Sea catchment accounts for 3 to 30% of the net ecosystem C exchange, implying that weathering represents a significant sink of atmospheric CO_2 (Sun et al., 2017). In contrast, very few investigations dealt with the impact of chemical weathering on soil formation and CO_2 consumption in the environment underlain by intrusive mafic rocks such as gabbros and olivinite (Schroeder et al., 2000). There are relatively few studies on comparative weathering intensity of acidic versus basic silicate rocks at the catchment scale (Horton et al., 1999; Ibarra et al., 2016; Wymore et al., 2017). Notably, in the Karelia and

79 Kola provinces (northwestern Russia, see **Fig. 1**), cationic weathering fluxes estimated from
80 river water chemical compositions and daily discharges are among the lowest in the world:
81 TDSc = 0.33 and 2.3 t/km²/yr for granite and basaltic watersheds respectively (Zakharova et
82 al., 2007). Surprisingly for mafic rock dominated watersheds, the Baltic Shield values are
83 only half the value measured for central Siberian basalt (~5 t/km²/yr, Pokrovsky et al., 2005)
84 despite similar runoff but sizeable mean annual air temperature (MAAT) differences
85 (+1 ± 2°C in Karelia versus -9 ± 2°C in Central Siberia). Such a disagreement does not allow
86 reliable extrapolation of the widely used "temperature-basic rocks weathering intensity"
87 relationship (Dessert et al., 2003) for specific subarctic environments in the present and past.
88 Further, the temperature sensitivity of chemical weathering is recognized to be strongly
89 limited by river discharge and water residence time in soils (i.e., Maher, 2011; Maher and
90 Chamberlain, 2014; Ibarra et al., 2016; Raymond, 2017 and references therein). Therefore,
91 studying the weathering mechanisms at the soil and small catchment scales is necessary to
92 explain the differences in mafic rock weathering in Europe and Siberia and to reveal the
93 factors responsible for slower weathering rates under specific environmental conditions
94 present in NW Russia. Recently, strong interest to chemical weathering linked to widespread
95 deglaciation processes (i.e., Foster and Vance, 2006; Stroeven et al., 2016) has been focused
96 around Greenland Ice Sheets (Andrews et al., 2014; Hindshaw et al., 2014; Deuerling et al.,
97 2018), Arctic Islands (Hindshaw et al., 2016), and Iceland (Opfergelt et al., 2014; Hawley et
98 al., 2017).

99 In contrast to the western European boreal environments located in the vicinity of the
100 Baltic Sea that are housed in a relatively mild climate, the understanding of the geochemistry
101 of ecosystems situated along the Arctic sea coast, including the White Sea, still remains quite
102 poor. The Karelia and Kola provinces (northwestern Russia) belong to this zone and offer
103 possibility to study the weathering of the coexisting mafic (e. g. olivinite, gabbro-norite) and

felsic (e. g. gneiss, granite) rocks within a relatively small and therefore easily accessible spatial scale. The region is characterised by the presence of abundant glacial moraine and till deposits. In Finland, different genetic moraine types (e. g. ground moraine, Rogen moraine, Pulju moraine, Sevetti moraine, Kianta moraine, De Geer moraine, etc.) were determined according to the classification given by Hättestrand (1997) and their geochemistry, mineralogy and morphology were extensively studied (e.g., Peuraniemi, 1982; Zilliacus, 1989; Peuraniemi et al., 1997; Sarala, 2005, Lunkka et al., 2013). The chemical and mineralogical composition of the moraine that covers the study area (northern and southern Karelia) suggest it was formed from Quaternary deposits of Pleistocene age (Evdokimova, 1957; State Geological Map of Russian Federation, 2001). Soil ages in this zone are supposed to be around 10 Ky. According to Thiede et al. (2001), Karelia and the Arkhangelsk regions were covered in ice sheets only during the late Weichselian glaciation phase (i. e. 17-15 Ky). Supposedly, during this period the soil erosion process was so important that almost all the soil cover disappeared in contrast to more southern regions (Salminen et al., 2008) where soil profile ages vary from 60 to 150 Ky.

Cool and humid boreal regions of Europe are dominated by podzolic soils extensively described in Russia (Dokuchaev, 1880; Ponomareva, 1964) and western Europe (e.g., Muir, 1961; Anderson et al., 1982; Buurman, 1984; Righi and Chauvel, 1987; Lundström, 1993; Courchesne and Hendershot, 1997, van Breemen and Buurman, 1998; Lundström et al., 2000, 2000a; Buurman and Jongmans, 2005). Podzols are typically found on coarsely textured base-poor parent materials such as sands and sandy tills, and are often located in Precambrian Shield granitic/gneissic environments (Lundström et al., 2000). However, podzol type soils were also described in mafic and ultramafic environment under boreal climate (e. g. Lesovaya et al., 2008; Salminen et al., 2008). The occurrence of podzol type soils over mafic rocks is also suggested in the World Reference Base for soil Resources (IUSS Working Group WRB,

129 FAO, 2006); however, considering the most used taxonomic systems criteria, only few of
130 those podzol type soils which developed over mafic rock could be classified as a true podzol.
131 Indeed, even if soils show a podzol like morphology (i. e. occurrence of an eluvial "albic"
132 horizon overlying a reddish-brown illuvial "spodic" horizon), the pH of these soils are usually
133 too high compared to classic podzols (D'Amico et al., 2008). According to D'Amico et al., in
134 such a case, the podzolisation process is favoured by the occurrence of quartz-rich
135 allochtonous material such as aeolian deposit or till. The question of the role of moraine
136 deposits in boreal podzol pedogenesis under a granitic environment was also raised by a
137 number of recent works devoted to the study of mineralogical and major and trace element
138 composition (as well as calculation of weathering losses) of podzols and spodosols developed
139 on granite-gneiss glacial moraine deposits in northern Europe (Öhlander et al., 1991, 1996,
140 2003; Giesler et al., 2000; Melkerud et al., 2000; Olsson and Melkerud, 1989, 2000; Land and
141 Öhlander, 2000; Land et al., 1999, 1999a, 2002; Tyler, 2004; Starr and Lindroos, 2006).
142 Lundström et al. (2000a) reported results of a multidisciplinary study (combining
143 geochemical, mineralogical, micromorphological, microbiological, hydrochemical and
144 hydrological investigations) aimed at testing various mechanisms (adsorption/precipitation
145 versus biodegradation) controlling the formation of podzols in glacial till context. Clay
146 mineralogy and chemical weathering of soils in a recently deglaciated arctic-alpine
147 environment in Sweden were studied by Allen et al. (2001). The authors suggest that the
148 occurrence of mixed layer minerals could be a tracer of parental rock weathering in soils
149 affected by moraine deposits. Contrastingly, Akselsson et al. (2006) found that there is no
150 relation between elemental content and mineralogy of till and bedrock mineralogy for
151 podzolic soil in southern Sweden and concluded that the information on the bedrock is not
152 sufficient for prediction of till mineralogy.

153 In northwestern Russia chemical and mineralogical composition of soils developed on
154 nepheline syenite, amphibolite and metamorphized diabase that were affected by moraine
155 deposition were recently studied by Lesovaya et al. (2008). These authors argued that soil
156 profiles became thicker and showed notable clay mineral transformation when allochtonous
157 moraine material is intermixed. In a more recent study (Lesovaya et al., 2012), the same team
158 studied chemical weathering processes of mafic rocks in the polar Ural and emphazised
159 weathering of smectite and secondary iron hydroxide accumulation in relation with
160 acidification processes (biota effect) wich are unusual in ultramafic environement. Thus,
161 despite these aforementioned studies on soil formation and chemical weathering processes in
162 boreal environment, there is still a lack of studies devoted to soil forming processes on mafic
163 rocks and related river hydrochemistry under glacial moraines.
164 Towards improving our understanding of mafic rocks weathering in boreal climate, we
165 use a multidisciplinary approach which is comprised of studying the geochemical migration
166 and partitioning of major and trace elements between different reservoirs (rocks and soils),
167 major and trace elements analysis, Sr and Nd isotopic measurement, and mineralogical
168 investigation. We aimed at characterizing rock weathering rates and adjacent rivers
169 hydrochemistry in order to understand the soil forming processes on basaltic rocks in the
170 boreal zone influenced by glacial moraine.
171 For this, we studied mafic and felsic rocks, as well as soil and water samples collected
172 within the Kivakka (northern Karelia) and Vetreny Belt (southeastern Karelia) magmatic
173 formations that are bounded by Archean age crystalline granitic rocks. The main questions we
174 attempt to answer in this study are: *i*) "to what degree the presence of a granitic-gneissic
175 moraine can modify the weathering features of basic rocks and degree of element leaching
176 from these rocks?", *ii*) "what are the differences between different mafic rock (gabbro,
177 norites, peridotites, olivinites, and basalts) degree of alteration in soils under the same

178 environmental conditions (climate, vegetation)?" and *iii*) "how contemporary weathering
179 processes are reflected in surface and soil water chemical compositions?"
180
181 **2. Geological and geographical setting**
182 The Vetreny Belt paleorift and the Kivakka layered intrusion are situated in the
183 Karelian region of northwestern Russia and exhibit similar geological, climatic, and
184 hydrological conditions. The main difference between these two sites is the nature of their
185 mafic rocks: gabbro-norite (peridotite) create the Kivakka intrusion and basalts with some
186 olivinites create the Vetreny Belt.
187
188 *2.1. Lithology, soils and vegetation*
189 The Karelian region is situated in the north-western part of Russia, bordering Finland
190 to the west, Lakes Ladoga and Onega to the south, and the White Sea – an extensive gulf of
191 the Arctic Ocean – to the east. Largely a hilly plain, the region has mountains in the west with
192 elevations up to 600 m. The lowest elevations are near the White Sea and the many lakes that
193 have filled depressions scoured across the surface during the last glaciation period. The relief
194 of Karelian zone was formed under the influence of glaciation which occurred at least 3 times
195 during Pleistocene (Reimann and Melezhik, 2001) with and the last glacier disappearing about
196 20-10 thousand years ago.
197 The study area is also a part of the Eastern Fennoscandian Shield. A simplified map of
198 the two chosen sites along with sampling points and some geological information are given in
199 **Fig. 1**. Quaternary deposits consist primarily of coarse-grained and sandy till or glaciofluvial
200 deposits showing well-developed podzol profiles. Detailed information of major and trace
201 element composition of volcanic rocks and rock-forming minerals utilized in this work can be
202 found elsewhere (Amelin and Semenov, 1996; Koptev-Dvornikov et al., 2001; Bychkova,

2003; Bychkova and Koptev-Dvornikov, 2004; Bychkova et al., 2007 for the Kivakka layered intrusion; Kulikova and Kulikov, 1981; Ryabchikov, 1988; Puchtel et al., 1996, 1997; Kulikov, 1999; Kulikov et al., 2005 for the Vetreny Belt; Lobach-Zhuchenko et al., 1986, 1993; and Bibikova et al., 2005 for the Archaean granitic and tonalitic gneisses surrounding the chosen intrusions).

The main part of the studied zone belongs to a boreal taiga forest ecosystem with pine, fir, birch, ericaceous species, and mosses that cover more than 80 % of the territory. Approximately 20 % of the territory is covered by wetlands that were developed on thick peat and gley-podzol soils. On well-drained territories alluvial-ferruginous-humic and alluvial-humic podzols prevail. They are developed under pine- and spruce-pine forests with moss-fruticulose cover. The soil depths in the region vary from 30-40 cm in the northern part and 60-85 cm in the southern part of Karelia. On the hill tops (100-200 m) soil depths do not exceed 10-20 cm. Ferruginous podzols are remarkable for high acidity, especially in superficial horizons (Lundström et al., 2000a and references therein). Soils are partly developed on a glacial granite moraine which consists mainly of sand and loamy sand with gravel and boulder inclusions. The glacio-lacustrine and lacustrine as well as fluvio-glacial deposits commonly form in lenses and are wide spread (Zakharova et al., 2007).

2.1.1. Vetreny Belt paleorift

The Vetreny Belt (63°46'N – 35°48'E) (**Fig. 1**, left) is situated in the south-eastern part of the Baltic Shield on the territory of the south-eastern Karelia and Arkhangelsk regions. It occupies a territory of approximately 5200 km^2 and can be traced from Lake Vyg southeastward over a distance of more than 250 km. Its width increases from 15 to 85 km to southeastward where it plunges beneath Paleozoic cover of the Russian platform and extends further southeast (Kulikov et al., 2003). A detailed description of the Vetreny Belt suite is

given by Puchtel et al. (1997) who also suggested that massifs like Kivakka layered intrusion have an origin related to the Vetreny Belt volcanic and plutonic rocks. The Vetreny suite consists entirely of a thick unit of basaltic komatiites belonging to the Sumian and younger groups in the area (Kulikov and Kulikova, 1982). The isotopic dating of the Vetreny belt yielded the following ages: 2449 ± 35 Ma and 2410 ± 34 Ma (Sm-Nd), 2424 ± 178 Ma (Pb-Pb), 2437 ± 4 Ma (U-Pb) (Puchtel et al., 1997).

2.1.2. Kivakka layered intrusion

The Kivakka pluton (66°12'N – 30°33'E) (**Fig. 1**, right) is located in northern Karelia and belongs to a complex of layered peridotite-gabbro-norite intrusions in the Olanga group that hosts migmatized biotite and amphibole gneisses, granite-gneisses, and granodiorite-gneisses of Late Archean age (Lavrov, 1979; Amelin et al., 1995). In addition to the Kivakka pluton, the group includes the Lukkulaisvaara and Tsipringa massifs (Shmygalev, 1968; Lavrov, 1979; Klyunin et al., 1994; Semenov et al., 1995; Amelin and Semenov, 1996). All of these are spatially restricted to an east-west trending regional fault zone and comprise the eastern branch of an extensive belt of layered massifs whose western branches continue across Finland (Alapieti, 1982). Detailed geological and petrological descriptions of the Kivakka layered intrusion can be found in the work of Koptev-Dvornikov (2001). The isotopic dating of the massif yielded the following ages: 2420 ± 23 Ma (Sm-Nd), 2445 ± 3.4 Ma (Zr) and 2444 ± 1 Ma and 2445 ± 2 Ma (Amelin and Semenov, 1990, 1996; Barkov et al., 1991; Balashov et al., 1993).

2.2. Climate and hydrology

The climate of most of the territory is mildly cold, transitionining between oceanic and continental, with a dominant influence of the Arctic and Northern Atlantics. Snow period lasts

from October through April-May with snow cover thickness ranging from 70 up to 110 cm. Mean annual temperature is close to 0°C but extremes can reach as high as +35° and as low as -35°C in summer and winter periods, respectively. Mean precipitation amount is between 400 and 600 mm/yr.

The region has a well-developed river network that flows via a system of glacial lakes. Chemical composition of river water in Karelia is determined by chemical weathering of silicate parent rocks of the Baltic crystalline shield, quaternary deposits, and the presence of numerous peatlands. Typical values of total dissolved solids (TDS) for this region are 15-30 mg/l (Maksimova, 1967; Zakharova et al., 2007) and the concentration of suspended matter in the river is very low. The study region can be considered as pristine, although some influence from Kola peninsula smelters can be pronounced via long-range atmospheric pollution (i. e. de Caritat et al., 2001).

3. Materials and methods

3.1. Sampling of rocks, soils, surface waters and soil pore waters

A list of soil, water, and soil water samples as well as their bedrock composition is presented in **Table 1**. For both soils and waters, series named "V" and "K" correspond to samples collected within the Vetreny Belt paleorift or Kivakka layered intrusion zones, respectively. Three altered rocks – an Archean gneiss, basalt, and peridotite – were sampled within the Vetreny Belt intrusion zone while two other basic rocks – a gabbro-norite and olivinite – were sampled from Kivakka layered intrusion in order to investigate formation of secondary phase minerals in thin sections. Ten soil profiles, five from each study site and five from each type of mafic and felsic parent rocks were sampled for pedological, mineralogical and chemical analysis (see **Table 1** for description and **Table SI-1** of **Supplementary Information 1** for chemical composition of soils).

278 Small and large rivers, as well as several wetlands and soil pore waters draining
279 through mafic and felsic rocks were sampled during extensive field campaigns in July 2004
280 and July 2006 for dissolved major and trace elements contents. Each location was sampled
281 only once. Three types of water were chosen for this study: river water, bog water, and
282 interstitial soil solutions draining from both felsic and mafic rocks (see **Table 1** for
283 description and **Table 2** for chemical composition of waters).
284
285 *3.2. Analytical techniques*
286 *3.2.1. Mineralogical and chemical analysis of rocks and soils*
287 Mineralogical studies on altered rock material were made on polished consolidated
288 thin sections using optical microscopy, scanning electron microscopy (SEM GEOL 6360LV
289 coupled to EDS PGT SDD SAHARA) including X-ray microanalysis, and electron
290 microprobe analysis (CAMECA SX50) in the GET laboratory (Toulouse). Modal composition
291 of the different altered rock samples was calculated by using structural formulae of minerals
292 and chemical composition of parental rocks and was coupled with SEM information. Analysis
293 of clays in soil sample K-14 (C horizon) was performed by transmission electron microscopy
294 (TEM) in the CRMCN laboratory, Paul Cézanne University, Aix-Marseille III, France.
295 The individual composition of soil minerals was determined by SEM with EDS on soil
296 grain thin sections. Afterwards, a structural X-ray diffraction analysis (XRD) was performed
297 on soil clay fractions in the GET laboratory (Toulouse). Clay fraction (i. e. < 2 µm grain size)
298 was separated by decantation in water column. Furthermore, structural XRD analysis
299 performed on INEL G3000 Cu $K\alpha_1,\alpha_2$, oriented samples were prepared by dropping of
300 < 2 µm suspension on a glass plate and drying it at room temperature. Standard treatment
301 (H_2O, ethylene glycol, and heating at 500°C) was employed to assess the interlayer distances
302 of clay minerals.

After crushing, pulverization, and homogenization, soil samples were digested in H_2O_2 at 25°C for 24 h and then in HF-HNO_3-HCl on a hot plate at 60-120°C in Teflon beakers in a clean room (classes between 5 and 7 according to the ISO 14644-1 standard). The validity of total chemical analysis for soils was verified by applying the same procedure for international geostandards BE-N (i. e. basalt), GA and AC-E (i. e. granites) for rocks, and LKSD-1 (i. e. lake sediment) for soils. Trace elements in rocks and soils were analysed by ICP-MS with an uncertainty < 10 % for the elements presented in this study. Indium and rhenium were used as internal standards. Major elements in soils were analysed by ICP-AES method in SARM laboratory (Nancy, France) and ALS Chemex laboratory (Vancouver, Canada). The analytical error of these measurements was in the range 5-10 %.

Total organic carbon (TOC) was analysed in dried soils by a Horiba carbon/sulphur analyzer EMIA-320V with an uncertainty better than 10 %. Soil pH was measured in deionised water suspension according to international ISO norms for measuring soil pH (AFNOR, 1996, ISO 10 390). The accuracy of measurements was ± 0.05 pH units.

3.2.2. Chemical analysis of river, mire and soil pore waters

Physico-chemical parameters of unfiltered water samples (pH, temperature (± 0.2°C), and electrical conductivity) were measured in the field. The pH was measured using a combined Schott-Geräte electrode calibrated against NIST buffer solutions (pH = 4.00 and 6.86 at 25°C), with an accuracy of ± 0.02 pH units. Samples were collected from near the middle of the flow channel, using 1-l high-density polyethylene (HDPE) containers held out from the beach on a non-metallic stick. Vinyl gloves were always used during handling of the samples. The water samples were immediately filtered through sterile, single-use Minisart® filter units (Sartorius, acetate cellulose filter) with pore sizes of 0.45 µm. The first 200 ml of the filtrate were systematically discarded. Filtered solutions for cations, trace element and Sr

328 isotope analyses were acidified (pH = 2) with ultrapure double-distilled HNO_3 and stored in
329 HDPE bottles previously washed with ultrapure 0.1 M HCl and rinsed with MilliQ deionized
330 water. Filtered water samples for anions were not acidified and stored in HDPE bottles
331 previously washed according to the above-described procedure for cations. Samples for
332 dissolved organic carbon (DOC) were collected in pyrolysed (550°C) Pyrex test tubes.

333 Soil pore waters were extracted from humid soil horizons in the field using a Ti
334 pressure device. This titanium vessel has a 50 mm diameter, 150 mm length, and a special
335 thread allowing it to reach 20 000 kg/cm^2 pressure. Depending on saturation state of soil
336 samples, 10 to 50 ml of solution was collected and filtered through a 0.45 µm filter. After
337 each extraction, the vessel and its compartments were thoroughly washed with river water,
338 and afterward, by 100 to 200 ml with distilled water. Before and after fieldwork, blank
339 samples were run by filling the pressure system with MilliQ water at neutral pH and letting it
340 to react for 24 h. No detectable contamination of major and trace elements and DOC was
341 observed.

342 Major anion concentrations (Cl, SO_4, F, NO_3, PO_4) were measured by ion
343 chromatography (HPLC, Dionex ICS 2000) with an uncertainty of 2 %. Calcium, magnesium,
344 sodium, and potassium concentrations were determined using an atomic absorption
345 spectrophotometry (AAS) Perkin-Elmer 5100PC spectrometer with an uncertainty of 2 %.
346 Aqueous silica concentration was determined by standard colorimetry (molybdate blue
347 method) with an uncertainty of 2 % using Technicon automated analyzer. Alkalinity was
348 measured by potentiometric titration with HCl to pH = 4.2 using Gran method with detection
349 limit of 10^{-5} M and an uncertainty of 2 %. DOC was analyzed using a Carbon Total Analyzer
350 (Shimadzu TOC 5000A) with a detection limit of 0.1 µg/l and an uncertainty better than 3 %.

351 Trace elements were measured without preconcentration by ICP-MS (Elan 6000,
352 Perkin Elmer and 7500ce, Agilent Technologies). Indium and rhenium were used as internal

353 standards. The international geostandard SLRS-4 (Riverine Water Reference Material for
354 Trace Metals certified by the National Research Council of Canada) was used to check the
355 validity and reproducibility of each analysis. A good agreement between our replicated
356 measurements of SLRS-4 and the certified values was obtained (relative difference < 5 %).
357
358 *3.2.3. Isotope analysis of surface waters and soils*
359 Strontium and neodymium isotopic ratios were measured by thermal ionization mass
360 spectrometry (TIMS) (Finnigan Mat 261) preceded by chemical separation, involving the
361 dissolution of the sample and chemical extraction of Rb, Sr, Sm and Nd by ion exchange
362 chromatography using three chromatographic materials Sr.Spec, TRU.Spec and Ln.Spec, and
363 HF, HNO_3 and HCl acids in a clean room. Data correction was based on the systematic
364 analysis of the NBS 987 standard for Sr and the La Jolla standard for Nd (i.e., correction for
365 instrumental mass fractionation based on hourly drift at the day of analyses). During this
366 work, the average $^{87}Sr/^{86}Sr$ for NBS 987 standard was 0.710250 ± 0.000010 (4 measurements)
367 and 0.511834 ± 0.000006 for $^{143}Nd/^{144}Nd$ (1 measurement).
368
369 **4. Results**
370 *4.1. Bedrock and soil mineralogy and chemistry*
371 The mineralogy and chemistry of studied rocks are described in **Supplementary**
372 **Information 2**. Mineral composition of solid material was characterized by structural X-ray
373 analyses of fine (< 0.1 µm, 0.1-2 µm and > 2 µm) and bulk fractions of 10 soil profiles:
374 samples V-4, V-7 (basalts), V-9, V-16 (gneisses), V-15 (peridotites, olivinites) and K-7, K-29
375 (gneisses), K-14 (olivinites), K-37 (gabbro-norites). Clay mineralogy results presented in this
376 study were obtained on soil samples having enough fine fraction for analysis. However, in
377 boreal podzols, the clay fraction is generally known to be < 5 % (Melkerud et al., 2000;

Mokma et al, 2004; Allen et al., 2001). Although peak intensities in the diffractograms varied somewhat as a function of depth, the < 2 µm fractions from soils developed on basic rocks indicated that quartz (all samples except K-14-C and V-15-O/A), feldspar (all samples except K-14-B_1 and -C and V-15-O/A), amphibole (all samples except K-14-B_1), illite (all samples), chlorite (all samples except K-37-A, V-16-E and -B, V-9-A and V-15-O/A), vermiculite (K-7, K-14, K-37-B_1 and -B_2, V-16-B, V-15), as well as interstratified layers illite/vermiculite (K29-O/A), smectite (K-37-B_1, V-4-E and V-15-O/A) and amorphous phases (K-29, V-16, V-7 and V-9) were the major clay-fraction constituents (**Table 3**). Amorphous aluminosilicates (i. e. imogolite), chlorite, regular interstratified layer mica/vermiculite (25 Å) were found in soil profile K-29 developed on granite-gneiss which is comparable to the clay fraction composition of podzols developed on granite-gneissic rocks in southern Sweden described by Schweda et al. (1991) and in northern Sweden described by Land et al. (1999). Hydrobiotite, a mineral containing regularly interstratified layers of biotite and vermiculite (Sawhney, 1989, Murashkina et al., 2007), was indicated by a peak at 12 Å in felsic soil K-29.

The analysis of the clay fraction in K-14 (**Fig. 2)** indicated the presence of vermiculite (occurrence of a 14.4 Å (7.3 Å) peak on the air-dried pattern, expandable on the ethylene-glycol pattern and collapsed on the heated pattern), illite (10 Å) and amphibole (8.4 Å). The analysis of V-15 peridotite (**Fig. 2A)** showed the presence of both of expandable vermiculite and smectite (vermiculite predominant), and an interstratified layer of illite/vermiculite (23.4 Å). The TEM investigations on the K-14 sample over olivinite from the Kivakka intrusion allowed for acquisition of detailed information on the nature of vermiculite formed in the C horizon of this soil (**Fig. 2B**). These results confirmed the presence of Mg-vermiculite together with chlorite and amphibole which also contained Mg.

Optical and SEM observations on consolidated thin sections of structurally preserved soil samples from different horizons revealed the presence of quartz and feldspar in almost all

403 studied soil profiles developed on basic rocks: gabbro-norite, olivinite, and peridotite, with the
404 exception of the C horizon of K-14 (soil over olivinite) and the O/A horizon of V-15 (soil
405 over basalt). Zircon was found in soils developed on granite-gneisses (K-7, B horizon; K-29,
406 C horizon, V-16, E horizon). Morphological observations of soils by SEM carried out during
407 this study reveal the presence of etch pits corrosion on the surface of zircon and feldspar
408 (**Fig. 3 A, B**) together with newly-formed matter visible as a coating on quartz, plagioclase
409 and pyroxene surfaces (**Fig. 3 C**). The pH (H_2O) of soils developed on felsic rocks varied
410 between 3.43 and 7.60, and those on basic rocks between 3.82 and 8.74, being the most acid
411 in the surface organic rich soil horizons. The high pH found for V-4 and K-14 soils could be
412 attributed to the mafic nature of the parental rock. Podzolisation process is favoured within
413 low pH environment which is usually the consequence of pedogenesis on acid rocks under
414 deep and acid litter. In this context, the pH (H_2O) measured for the V-16-B and K-8-B
415 samples are problematic (pH is too basic for a podzol type soil). The TOC concentration
416 ranged from 7.7 to 42.1 % wt in organic surface horizons (O/A), and from 0.15 to 3.5 % wt
417 for deeper horizons (E, B and C).

418 Chemical analysis of soils was performed on bulk fractions (including gravel).
419 Observations of elements concentrations along the soil profiles (not shown) show that all soils
420 developed on felsic rocks exhibited higher content in Si, K (except K-29), Al (except K-7)
421 and Na, and lower content in Ca (except K-29), Fe and Mg with respect to their parent rock.
422 Podzol V-7 developed on basic rocks showed relatively higher content in Si, Al, Na and K
423 than its parent rock similarly to the soils developed on felsic rocks (V-9, K-8, K-29). K-14
424 and K-37 exhibit low Si, Al and Na content compared to olivinite or gabbro-norite. Higher
425 content in K in the surface horizon compared to the parental rock was observed for all soils
426 except K-14, K-29 and V-15. Almost all soils developed on basic rocks showed lower content
427 in Fe (except K-14) and Mg (except V-9 and V-15) compared to their respective parent rock.

Photos of podzols V-4, K-14 and K-37 developed on basalt, olivinite and gabbro-norite, respectively, and regosol K-29 over gneiss are presented in **Fig. 4**. A diagram of weathering intensity scale (WIS) used to evaluate the chemical index of alteration (Meunier et al., 2013) allows to see how the moraine influences the chemistry of soils (**Fig. 5**). Regardless of the parent rock, the majority of soil samples are located in the "felsic" domain.

4.2. REE distribution pattern

The upper crust (Taylor and McLennan, 1985) normalized rare earth elements (REE) patterns for selected soil samples are plotted in **Fig. 6**. REE patterns of soil horizons are different from those of the corresponding parent rocks. A slightly positive europium anomaly can be observed in the majority of soil horizons and is likely to be related to the presence of feldspar in the soil-rock system. Eu/Eu^* (**Table SI-1**) is calculated using the formula (Condie, 1993):

$$Eu/Eu^* = Eu_N/(Sm_N \cdot Gd_N)^{1/2}$$

where $Gd = (Sm \cdot Tb^2)^{1/3}$. The ratio is within the range 0.87-1.05 for soils on basic rocks for both the Vetreny Belt and the Kivakka intrusion, and 0.88-1.18 and 0.91-1.09 for soils on felsic rocks for the Vetreny Belt and the Kivakka intrusion, respectively. It can be observed that the ratios are quite similar for both felsic and mafic soil-rock systems, again confirming the influence of exterior moraine deposits. This result is further corroborated by extended upper crust (UC) normalized diagrams that include all major and trace elements (**Fig. 7**). The soils of felsic and mafic origin from the Kivakka intrusion site (samples K-7, K-8, K-29 and K-37) are shown in **Fig. 7 A** and for soils from the Vetreny Belt site (samples V-7, V-9, V-16, V-4 and V-15) are shown in **Fig. 7 B**. It can be seen that all soils from the Kivakka intrusion zone exhibited quite similar upper-crust normalized trace elements patterns independent on their parent rock. The soils were generally depleted in most elements compared to the upper

crust: Li, Sc, Mn, Co, Ni, Cu, Zn, As, Rb, Y, Zr, Nb, Mo, Cd (except surface horizons O/A of soils K-7, K-29 and K-37), Sb, Cs, Hf, Ta, W, Tl, Pb, Th, U. For these elements surface horizons O/A appear to be more depleted than the deeper ones. Olivinitic soil K-14 (not shown) exhibited a slightly different pattern, being less depleted in the above mentioned elements relative to the upper crust and enriched in Cr, Co, Zn and Ni, in accord with these elements elevated concentration in the source rocks. For some soil samples a slight enrichment in V (samples K-7-B, V-9-A, V-15-O/A), Cr (K-37 all horizons, V-15-O/A (significantly enriched), V-9-A, V-7-B), Sr (K-29, E and C horizons), Cd (K-7-O/A, K-37-O, V-9, O and A horizons, V-7-E) and Sb (K-7-O/A, K-29-O/A, V-9-O) relative to the upper crust can be observed. The last observation is also true for V-15 sample developed on ultramafic rocks. The soils from the Vetreny Belt zone (**Fig. 7 B**) exhibited similar pattern independent on their parent rocks, and most of them are depleted in Sc, Ti, Co, Ni, Cu, Zn, Ge, Rb, Sr, Y, Zr, Nb, Cs, Hf, Ta, Th, U and significantly in Pb compared to the upper crust. The surface horizons O/A were depleted in V, Cd and Sb. A-horizon of soil V-9 and V-15 were enriched in Sc, V, Cr, Co, Ni, Cd, and all soils were significantly enriched in Tl with respect to the upper crust. Overall, results on TE partitioning in soils corroborate the previous conclusion on the dominant role of glacial deposits on soil chemistry both on mafic and felsic rocks. Taken together, all soils from the Kivakka intrusion and the Vetreny Belt zone exhibit quite similar UC-normalized trace element patterns independent on their parent rock. This confirms the dominant role of glacial deposits on soil chemistry for both mafic and felsic rocks, i.e., the glacial erosion has predetermined the soil development.

4.3. Hydrochemistry of rivers and soil porewaters

Measured pH and temperature, dissolved organic carbon (DOC) concentration, major and some trace elements concentrations (Al, Fe, Sr and Rb), as well as $^{87}Sr/^{86}Sr$ isotopic ratios

478 for river and stagnant mire waters are presented in **Table 2** for both the Kivakka intrusion and
479 the Vetreny Belt zones. The studied waters were essentially of neutral pH varying from 6 to
480 7.5. However, some surface organic rich waters and bog waters were more acidic with pH
481 decreasing to 4.5-5.5. Bicarbonate ion concentrations ranged from 1.8 to 40.2 mg/l for rivers
482 draining basic rocks and from 8.3 to 80.2 mg/l for rivers draining felsic rocks. In surface
483 wetlands and interstitial waters from soils developed on basalts, the alkalinity ranged from 2.2
484 to 8.0 and from 1.8 to 29.9 mg/l, respectively. The majority of surficial fluids exhibited high
485 concentrations of dissolved organic carbon between 5 and 40 mg/l.

486 The composition of the dissolved load of most rivers reflects the weathering of silicate
487 rocks because the total dissolved solids (TDS) expressed as a sum of major inorganic species
488 concentrations (Na, Ca, K, Mg, Al, Fe, H_4SiO_4, Cl, NO_3, and SO_4) was low (between 10 and
489 30 mg/l). These measurements are comparable with previous results on Karelia region
490 (Feoksitov, 2004, Zakharova et al., 2007). Rivers analyzed in this study had an average Si
491 concentration of around 4 mg/l (3.6 ± 0.9 and 4.3 ± 1.3 mg/l for rivers draining felsic and
492 mafic rocks, respectively) which constitutes only 30 % of the TDS. Calcium and sodium were
493 dominant among cations in these waters.

494 The concentration of major dissolved cations in surface (river and bog) water for both
495 the Vetreny Belt and the Kivakka intrusion zones (average values in µmol/l are given in
496 brackets) followed the order Ca (336) > Mg (116) > Na (77) > K (16) for waters draining
497 through felsic rocks and Mg (95) > Ca (77) = Na (77) > K (7) for those draining through
498 mafic rocks. Potassium and sodium concentrations (16 µmol/l and 90 µmol/l, respectively)
499 were comparable with those reported by Ingri et al. (2005) for a pristine boreal Kalix river
500 draining through a mixed felsic and carbonate-shale environment, whereas calcium content in
501 this study is higher than that of the Kalix river (149 µmol/l). We did not detect any systematic
502 difference in Mg concentration between felsic and mafic catchments; concentration varied

503 from 400 to 8000 µg/l within the Vetreny belt zone and from 100 to 13000 µg/l within the
504 Kivakka intrusion zone. Within the basic rocks catchments, we could not detect any sizeable
505 difference between waters draining through rocks of different composition (gabbro-norites,
506 olivinite, and basalts).
507
508 *4.4. Radiogenic isotope features*
509 Concentrations of Rb, Sr, Sm and Nd, and $^{87}Sr/^{86}Sr$ and $^{143}Nd/^{144}Nd$ isotopic ratios for
510 soils from the Vetreny Belt and the Kivakka intrusion are reported in **Table SI-1**. Peculiar
511 feature of soil and water geochemistry in considered zones is large variation of their Sr
512 isotopic composition (**Fig. 8**). For the Kivakka intrusion, soils developed on olivenite (K-14,
513 the deepest horizon) and TTG (K-29) have lower $^{87}Sr/^{86}Sr$ ratios (0.704) similar to parental
514 rock isotope ratios (Amelin and Semenov, 1996). An opposite tendency is obtained for other
515 soils developed on mafic and felsic rocks (**Fig. 8 A**). For example, $^{87}Sr/^{86}Sr$ ratios of the
516 samples K-37 (0.721-0.726) which was developed on gabbro-norites are similar to those of
517 felsic K-8 (0.721-0.725). These samples are enriched in Rb, and have the same $^{87}Sr/^{86}Sr$ ratio
518 as estimated by Land et al. (2000) for podzols developed on Quaternary till of granitic
519 composition in northern Sweden (0.721-0.727). Furthermore, soil horizons B_2 and C of
520 ultramafic sample K-14, and B_2 of mafic sample K-37 have similar pedological characteristics
521 to those of the B horizon of felsic sample K-7, and quite similar in isotope ratio ($^{87}Sr/^{86}Sr$
522 ~0.718 and $^{87}Rb/^{86}Sr$ ~0.6). The soils developed on mafic rocks from the Vetreny Belt zone
523 exhibited similar features with $^{87}Sr/^{86}Sr$ and $^{87}Rb/^{86}Sr$ isotope ratios higher than their source
524 rocks. This unambiguously suggests strong influence of external (moraine) deposits.
525 Concerning the isotopic composition of surface waters, the results demonstrate two similar
526 tendencies for both sites (**Fig. 8 B**): *i*) waters show higher Sr isotopic ratios (between 0.715
527 and 0.730) compared to rocks and rock minerals (between 0.705 and 0.713) within the same

range of $^{87}Rb/^{86}Sr$ ratios (from 0 to 0.4), and *ii*) Sr isotope ratios of waters are in the same range as soils (except for soil V-15 from Vetreny Belt site) although soils have higher $^{87}Rb/^{86}Sr$ ratios (0.3-0.75) than water (< 0.3). Thus, surface waters have a more radiogenic signature than parental rocks and primary minerals for "basic rock derived" samples.

5. Discussion

5.1. Moraine influence over the full depth of soil profile

5.1.1. Major elements

The occurrence of corroded zircon and feldspar and the evidence of clay mineral formation in those soils witness similar weathering processes on all types of parental rock. Etch-pitting of zircon is usually related to intense weathering processes, generally in tropical environment (e. g. Oliva et al., 1999). However, the lack of kaolinite neoformation and the persistence of amphibole and plagioclase feldspar in soils suggest not very intense weathering processes, consistent with the beginning of pedogenesis about 10 Ky ago. Our mineralogical observations of secondary phases are consistent with the presence of hydrobiotite, amorphous phases, smectite and K-feldspar over nepheline syenite in horizons C and B_2 as well as quartz and plagioclase in horizons B_1 and E described in mountainous tundra soils of northwestern Russia (Lesovaya et al., 2008). These results are also compatible with the clay fraction composition of soils developed on glacial moraines in Finland (gneissic moraine material) (Melkerud et al., 2000; Mokma et al., 2004) which includes quartz, plagioclase, K-feldpar, amphibole, chlorite, illite, mixed layer illite/vermiculite, and allophanes. Observed mixed layer chlorite/vermiculite is reported as a product of degradation of chlorite.

Classically, element depletion or enrichment in soils samples compared to respective unaltered rocks at the soil profile scale (i.e., mass balance approach) is estimated via element ratios with invariant low-mobility elements (i. e. Zr, Ti, Al, Th) in soils and rocks (**Table SI-**

553 **1**). Theoretical concentrations of major elements in soil profiles were systematically higher
554 compared to the parental rock for Na and/or K except for the B_1 and C-horizons in samples K-
555 14 (soil over olivinite, Kivakka intrusion) and V-15 (soil over peridotite, Vetreny Belt).
556 Moreover, the Zr/Ti ratio was not constant along the soil profiles as we observed a depletion
557 in Zr in O and A horizons and slight enrichment in B horizons. This may suggest that Zr or Ti
558 were not initially homogeneously distributed in soils or that Ti is not invariant in these
559 profiles. Potential Zr mobility in soils and the difficulty of using Zr as refractory element for
560 mass balance calculations are widely known (see recent work in Southern Spain, Ameijeiras-
561 Marino et al., 2017). Similar results were observed when using Al and Th as invariants. One
562 reason for this discrepancy can be the unusually high mobility of tetravalent elements in the
563 form of large-size organo-mineral ferric colloids whose presence is unambiguously
564 demonstrated in surficial waters of the Karelian zone (Pokrovsky and Schott, 2002;
565 Vasyukova et al., 2010). Using a CDF (chemical depletion fraction corresponding to the ratio
566 of chemical erosion rates to mineral supply rates) and chemical depletion fractions of
567 individual elements (Brimhall et al., 2001; Riebe et al., 2001 and 2004; Ferrier et al., 2016)
568 provide a more comprehensive approach of the chemical differentiation of the soil relative to
569 its parent material. In particular, CDF calculations allow to take into consideration external
570 element supply to the soils. Following Riebe et al. (2001, 2004), we calculated:

571 $CDF = 1- ([Ti]_{rock}/[Ti]_{soil})$ for the entire soil

572 $CDFx = 1-[([X]_{soil} / [X]_{rock}) \times ([Ti]_{rock} / [Ti]_{soil})]$ for individual element X

573 The CDF values using Ti as an invariant element (**Table 4**) showed important discrepancies
574 (i.e., values from 2 to -1670%) between different soil samples, including even the samples
575 taken within the same soil profile (K-8 and V-9 soil samples). These differences are not
576 linked to the nature of parental rock (i.e., mafic vs felsic). Positive CDF values is samples K-
577 7, K-14 and K-37 can be related to chemical losses from the parental material whereas

578 negative values in K-29, V-4, V-7 and V-16 can be attributed to fresh mineral supply to the
579 regolith. In soils where chemical dedudation seems to occur, positive CDF values should
580 decrease or remain constant from surface to depth. This was only observed in K-7 and K-37
581 soils. Thus, even for soil with positive CDF, the pathway and rate of chemical weathering
582 cannot be constrained. When chemical depletion fraction of individual element is considered
583 (**Table 4**), only K-14 B_1 and C horizons samples show positive values for all considered
584 element. Chemical depletion fraction of individual element confirm the relative enrichment of
585 soil samples in K and to a lesser extend in Na compared to the parental rocks. Some samples,
586 however, dis not exhibit relative enrichment in K (K-29 samples, V-9 A and V-15 O/A
587 horizon samples) or in Na (K-8 E, K-37 O, K-37 A, V-9 O, V-9 A and V-15 O/A horizon
588 samples) suggesting diverse origin of chemical supply to the soils. For example, K-29 soil
589 samples developed over felsic formation (i.e., granite/gneiss) showed negative CDF values in
590 Na, Ca, Al and Si. The enrichments in Si and Al are difficult to interpret as they mainly occur
591 in horizons presenting spodic properties that can result from element mobilisation within the
592 soil profile.

593 Another widely used proxy for chemical weathering intensity of source rocks for soils
594 and sediments is Chemical Index of Alteration (CIA; Nesbitt and Young, 1982; Fedo et al.,
595 1995, Li and Yang, 2010). It is calculated using the molar proportion of major elements, as
596 follows:

597 $$CIA = [Al_2O_3/(Al_2O_3 + CaO^* + Na_2O + K_2O)] \times 100$$

598 where CaO* used in the CIA calculation refers to CaO from the silicate fraction exclusively.
599 Basic rocks exhibit average CIA values (42 and 36 for Kivakka layered intrusion and Vetreny
600 Belt paleorift respectively) which are lower than the CIA of felsic rocks (CIA value of
601 archean granite ~50). It can be observed that the CIA of soils is not always higher than that of
602 their respective parent rocks (**Table 4**). The ratio $CIA_{soil\ sample}/CIA_{parent\ rock}$ is considered as a

603 proxy of the "weathering degree" of a soil. Some samples (V-15, V-9, K-8-C, all the K-29
604 samples) show CIA_s/CIA_r values lower than 1. Since the CIA calculation involves Al (thought
605 to be rather mobile during podzolisation) and K (a nutrient highly recycled by vegetation),
606 several hypotheses can explain this CIA value: 1) the loss of Al during weathering of K-
607 feldspars and downward migration due to podzolisation occurring mainly in E horizon; 2) the
608 accumulation of K from buried organic matter in the form of plant litter in the uppermost
609 organic-rich soil horizons, and 3) the input of K, Al, Ca, and Na from allochtonous sources.
610 Al loss during podzolisation usually affects the O, A and E horizons (Melkerud et al.,
611 2000; Olsson et al., 2000; Giesler et al., 2000); K incorporation may affect O horizon and the
612 effect of addition of allochtonous material depends on its origin (e. g. aeolian, morainic) and
613 composition. Incorporation of allochtonous material may actually lead to a "dilution" effect
614 thus underestimating the element content in the soil profile. As a result, even at zero level of
615 chemical weathering intensity, the presence of moraine or aeolian material can lead to an
616 under- or overestimation of the CIA depending on the chemical composition of the mineral
617 supply. Except in a few samples mentioned above, most soils developed on mafic rocks
618 showed $CIA_s/CIA_r > 1$ which is higher than that in soils over felsic formation ($CIA_s/CIA_r \sim 1$).
619 However, the dilution effect of the moraine was more pronounced for basic rocks compared to
620 acidic rocks because of the felsic dominant nature of the moraine.
621 Mineralogical studies performed on soils samples show the presence of ubiquitous
622 quartz (and in some soils, zircon) independent on the nature of the parental rocks. The size of
623 quartz grains varied from 10 to 450 µm and from 50 to 200 µm in soils developed on mafic
624 and felsic rocks, respectively, which precluded an aeolian origin of these quartz grains. In
625 contrast, quaternary (Pleistocene) deposits observed even in the deepest horizons of some soil
626 profiles (**Fig. 4 E**) confirm a strong moraine influence in this region. This moraine altered
627 significantly the chemistry of soils as it can be seen on the WIS diagram (**Fig. 5, Table 4**) that

628 take into account a silica component (Meunier et al., 2013). All studied rocks fall in their
629 respective "domain" within the WIS diagram. On the opposite, soils samples, whatever their
630 parental rock, fall in the "felsic domain", with the exception of the V-7 C, K-14, V-15 and V-
631 9 soils samples. Only the K-14 B1 and K-14 C samples are plotted close to the parental
632 olivenite suggesting a poor influence of allochtonous morainic material in K-14 soil
633 pedogenesis. In the felsic domain, TTG and glacial till (Lunkka et al., 2013) are chemically
634 similar with silica content lower than soils samples. This is coherent with chemical
635 weathering processes in cold environment wich involve relative enrichment in silica (quartz
636 preservation) in comparison with the alkaline earth elements (M^+ pole; $Na^+ + K^+ + 2Ca^{2+}$) or
637 the divalent metallic elements (R^{2+} pole; $Mg^{2+} + Fe^{2+} + Mn^{2+}$) that are lost from the soil
638 during pedogenesis. This trend is particularly pronounced when comparing E and B horizons
639 of podzolic soils on the WIS diagram. E horizons are systematically closer to the 4Si pole
640 than the B horizon. Such results suggest that, even if a strong morainic influence has
641 completely modified the mineralogical and chemical nature of the initial regolith, the soil
642 forming processes such as podzolisation occurring within these soils are similar and
643 consistent among different sites.
644
645 5.1.2. REE fractionation between rocks and soils
646 Five horizons of a soil developed on gabbro-norites (sample K-37 from the Kivakka
647 intrusion, **Fig. 6 A**) show enrichment in light rare earth elements (LREE) and depletion in
648 heavy rare earth elements (HREE) relative to the gabbro-norite. Enrichment in LREE was
649 also observed by Öhlander et al. (1996) in B-horizons of spodosols developed on felsic till in
650 northern Sweden, whereas E-horizons were depleted in all REE, with LREE being more
651 depleted than HREE. According to Öhlander et al. (1996), this secondary enrichment in B-
652 horizons could be caused by adsorption on secondary oxy-hydroxides, on clay minerals or

organic material, or by the precipitation of secondary LREE enriched phosphates. Note the higher affinity of LREE to adsorb on oxy(hydr)oxides and the tendency of HREE to form more stable dissolved complexes than LREE in solution (Bau, 1999) is in agreement with these tendencies.

Olivinite rock is enriched in HREE, and sample K-14 B_2 from the Kivakka intrusion (**Fig. 6 B**) is enriched in all REE relative to olivinite for all horizons of the soil profile. On the contrary, soils developed on felsic rocks (samples K-7, K-8, K-29 from Kivakka intrusion, **Fig. 6 C**) have inverted REE concentrations with respect to parental granite, all horizons are depleted in REE relative to the source rock. The REE patterns of soils developed both on mafic and felsic rocks in the Vetreny Belt zone (**Fig. 6 D**) demonstrate that soils developed on basalt (samples V-4 and V-7) are depleted in REE with respect to parental rock with the exception of the B horizon of V-7 which in slightly enriched in LREE. Soils over felsic rock are also more significantly depleted in all REE relative to the source TTG. However, it can be seen that patterns of soils with different origins (mafic or felsic) are quite similar. This is further illustrated in **Fig. 6 E** where the E or B horizons of different soils developed on both felsic (K-7, K-8, K-29) and mafic (K-14, K-37) rocks are plotted. It demonstrates that the REE fractionation in intermediate horizons in all studied soils is identical regardless of the underlying rock. This result is in agreement with observations of Lesovaya et al. (2008) on podzols and podzolized podburs on mafic substrates under the influence of glacial moraine deposits in mountainous taiga areas in northwestern Russia. According to these authors, the mineralogical effect of the admixture of gneiss-derived material is, in general, most pronounced in the E horizon.

678 *5.2. Actual weathering processes: waters versus soils and rocks*

679 A binary logarithmic diagram of the molar Ca/Na versus Mg/Na ratios in rocks, soils
680 and waters, including atmospheric precipitation shows that the Ca/Na ratio ranges from 0.2 to
681 8.6 and 0.25 to 5.8 for soils and waters, respectively (**Fig. 9**). The Mg/Na ratio varies between
682 0.15 and 8.9 for waters, and between 0.1 and 1.9 for soils; the highest ratio of 76.5 and 214.3
683 are for soil K-14 on olivinite (B_1 and C horizons, respectively). There is a good correlation
684 between Ca/Na and Mg/Na ratios in soils and rocks, and between surface waters and rocks.
685 The majority of samples from the Kivakka intrusion and the Vetreny Belt, exempting soils K-
686 29 (horizon E) and K-14 (horizons B_1 and C) which drop out of the tendency, are located on
687 the mixing line between silicate and carbonate end-members although no clear evidence of
688 carbonate phases was previously described for neither rocks nor soils and no carbonate
689 mineral was found within the resolution of XRD analysis of soils.

690 Lower Ca/Na and Mg/Na ratio for soils compared to rocks is consistent with on-going
691 chemical weathering, as calcium-rich phases usually weather more rapidly than sodium-rich
692 phases in silicate environments. In this regard, the addition of moraine material enriched in
693 Na (Na-K feldspar) can also explain this tendency. Lesovaya et al. (2008) observed the
694 presence of moraine admixtures in mafic rock-soil systems, expressed in the lower content of
695 calcium in the middle taiga soils of Karelia which could be due to the admixture of stable K-
696 Na feldspars**.**

697 Stream waters are known to have higher Ca/Na molar ratio than rocks and soils and
698 should exhibit lower Ca/Na ratio compared to parental rocks (Gaillardet et al., 1999; Oliva et
699 al., 2004). We observe different tendencies of water composition: surface waters are situated
700 either in the same region or are enriched in Ca or Mg compared to soils in the case of the
701 Vetreny Belt rock-soil-water system. For the Kivakka intrusion system the surface fluids are
702 located between the soil and rock reservoirs reflecting preferential mobilisation of sodium

703 relative to calcium or magnesium in these surface waters as compared to rocks. The waters
704 from the Vetreny Belt mafic rocks exhibit higher Mg/Na and lower Ca/Na ratios compared to
705 the Kivakka basic massif and surrounding felsic rocks, which is in agreement with higher Mg
706 concentrations in basalts of the Vetreny Belt (up to 20-25 % MgO in spinifex-like structures,
707 see Kulikov et al., 2005).

708 Unexpectedly, surface waters draining felsic environments show higher Ca/Na and
709 Mg/Na molar ratios than waters draining mafic rocks. This relative enrichment in Na with
710 respect to Ca and Mg in rivers from mafic watersheds compared to felsic watershed may be
711 explained by a higher mobility of sodium compared to Ca and Mg during the weathering
712 process and the retention of Mg and Ca during secondary phases forming. It is possible that
713 Ca and Mg, unlike Na, participate in secondary mineral formation such as Mg-vermiculite.
714 Some Ca and Mg rich phases (i. e. CaMg-amphibole) can also weather less rapidly than Na-
715 rich feldspar (Salminen et al., 2008). Soil K-14 which is over olivinite (B and C horizons)
716 exhibited a clear tendency of enrichment in Mg and Ca compared to Na during basic rock
717 weathering. This is consistent with the presence of Mg-vermiculite and CaMg-amphibole in
718 the clay fraction. The persistence of Ca-amphibole in such soils has been also observed by
719 Lesovaya et al. (2008).

720 Consistent with these chemical and mineralogical observations, the radiogenic
721 isotopes demonstrate two features of the water-soil-rock system development in NW Russia
722 (**Fig. 8**): (1) During different stages of weathering, easily weatherable and less radiogenic
723 minerals (secondary clays, carbonates) were strongly consumed throughout the full depth of
724 examined soil profile. This provided a more radiogenic Sr isotopic signature to most soils
725 developed on mafic rocks compared to that of the parent rocks which was especially
726 pronounced in the surface horizons. For both the Kivakka intrusion and the Vetreny Belt, we
727 observe a shift of $^{87}Sr/^{86}Sr$ from ~0.705 (rocks) to 0.715-0.725 (soils). The same behaviour

728 was reported for soils developed over basalts in Central Siberia (Bagard et al., 2013). Second,
729 all the granitic moraine in Karelian region had a more radiogenic signature than the studied
730 bedrocks. Isotope signatures of waters draining through both felsic and mafic zone reflect the
731 weathering of more radiogenic minerals. However, these radiogenic signatures are lower than
732 that reported by Land et al. (2000) for stream waters (~0.74) draining felsic rocks in northern
733 Sweden within the Kalix river watershed.
734
735 *5.3. Chemical weathering rates*
736 In general, the composition of surface waters does not reflect a purely felsic or mafic
737 source being similar in all waters, except for one Mg-rich surface water draining through
738 olivinite environment of the Kivakka intrusion (sample K-13-w). The surface waters draining
739 through both Kivakka and Vetreny Belt region are strongly oversaturated with respect to
740 $Al(OH)_3$, boehmite, gibbsite, halloysite, imogolite, kaolinite, ferrihydrite (factor 10 to 10^6),
741 and undersaturated with respect to amorphous silica, and close to saturation with quartz.
742 Apparently, the amorphous, organic-rich Al and Fe oxyhydroxides and silicates constitute a
743 major part of secondary phases in soils as is well known for boreal zone (Lundström et al.,
744 2000, Giesler et al., 2000). One particular feature in soil K-14 is the occurrence of Mg-
745 vermiculite and a high pH. Processes usually occurring in podzolic soils are rock dismantling,
746 Al- and Fe-organic complex formation, organic matter modification, oxidation of iron bearing
747 primary phases, and amorphous alumino-silicate precipitation. However, the podzolation
748 process is known to rarely produce any clay mineral formation and clays are relatively absent
749 (Mokma et al., 2004).
750 Only the K-14-C soil sample was not affected by moraine deposit, and thus, it can be
751 used in calculation of weathering rates of basic rocks. Our results give a long term TDS
752 weathering rate of 1184 eq/ha/yr for olivinite rock, which is 4 times higher than the long term

753 base cation flux (360 eq/ha/yr) and about 2 times higher than the actual TDS weathering rate
754 (~700 eq/ha/yr) estimated by Land et al. (1999) for granitic till in northern Sweden. This
755 value corresponds to a long term weathering rate of ~1.5 t/km²/yr which is lower than the
756 present day weathering rate estimated by Zakharova et al. (2007) and Pokrovsky et al. (2005)
757 for Karelian and Siberian mafic rocks (2.3 and 5-6 t/km²/y, respectively) but comparable with
758 chemical denudation rates of Canadian granites (0.35 to 1.55 t/km²/y for Slave Province vs
759 Grenville, Millot et al., 2002). Calculation of weathering fluxes were conducted for A and B_1
760 horizons and give values of 364 eq/ha/yr and 148 eq/ha/yr, respectively, which are consistent
761 with fluxes reported by Land et al. (1999) for the granitic till, and for podzol soils covered by
762 Norway spruce in Sweden (344 eq/ha/yr for Ca+Mg+Na+K, Simonsson et al., 2015). These
763 values are sizebly lower than the base cations release rate, calculated for similar
764 environmental context using various mineral dissolution models (1400-2700 eq/ha/yr,
765 Erlandsson et al., 2016).

766 Results of the present study demonstrate that the weathering rates of ultramafic rocks
767 are higher than those of the felsic till, but dominant moraine deposits in this region hide the
768 true magnitude of weathering processes. The dominant mechanism responsible for slowing
769 the rates of mafic rock weathering could be retention of Mg and Ca in soil are likely due to
770 precipitation of secondary phases such as Mg-vermiculite or adsorption on mineral, organic,
771 or organo-mineral phases.

772

773 **6. Conclusions**

774 A multidisciplinary study of mafic rocks weathering in the region affected by glacial
775 moraine deposits (northwestern Russia) demonstrated the following:

776 (1) Traces of chemical corrosion on the surface of zircons and feldspars along with the
777 presence of new-formed amorphous matter on the surface of quartz, plagioclases and

778 pyroxenes are evidence of similar weathering processes on all types of parental rock.
779 However, the lack of kaolinite neoformation and the persistence of amphibole and plagioclase
780 feldspar in soils suggest not very intense weathering processes, in accordance with a start of
781 pedogenesis about 10 Ky ago.

782 (2) The presence of quartz and zircon in soils developed on basic rocks, similarity of
783 REE patterns of intermediate and deep soil horizons both for felsic and mafic rocks, and the
784 isotopic signature of soils on gabbro-norite and olivinite similar to that of granodiorites raise a
785 question of the polycyclic nature of these soils (soil developed on fragments of already pre-
786 existing soil), and assume their "contamination" with exterior deposits such as granitic
787 moraine.

788 (3) The relative enrichment in Na with respect to Ca and Mg in rivers from both felsic
789 and mafic watersheds suggests a contribution from other sources than primary silicate
790 weathering reactions. We suggest that either Mg-vermiculite and Ca, Mg-amphibole
791 formation in soils limits Ca and Mg release to surface waters, or that there are highly
792 weatherable Ca- and Mg-rich minerals present in felsic rocks. These specific features should
793 be taken into account in estimation of mafic rocks weathering rates and calculations of
794 atmospheric CO_2 consumption for weathering in such a particular environment.

795 (4) The radiogenic isotopes of the water-soil-rock system development in NW Russia
796 demonstrated *i*) preferential removal of easily weatherable and less radiogenic minerals
797 throughout the full depth of soil profile, and *ii*) more radiogenic signature of the granitic
798 moraine compared to mafic and felsic bedrocks.

799 (5) In the cold subarctic climate, even thin deposits of glacial till moraine are capable
800 of "protecting" mafic rocks from direct chemical weathering. As a result, over 10 000-
801 15 000 years of exposure after the last glaciation, full weathering soil profiles on basic rocks
802 could not be established.

(6) The weathering rates of ultramafic rocks are higher than those from felsic till, but widespread moraine depositions in this region hide the magnitude of weathering processes. These findings may have broad applications for reconstructing paleo environments and quantifying the true capacity of igneous silicate rocks to absorb CO_2 during weathering in high latitude regions.

Acknowledgements

Authors are grateful to F. Candaudap, Th. Aigouy, Ph. and F. de Parceval, and P. Brunet for analytical support. C. Benker is thanked for thorough English proofread. Partial support from the TSU competitiveness improvement programme Project N 8.1.04.2018 is acknowledged.

References

AFNOR, 1996. Qualité des sols. Recueil de normes Françaises, Association Française de Normalisation, Paris.

Akselsson, C., Holmqvist, J., Kurz, D., Sverdrup, H., 2006. Relations between elemental content in till, mineralogy of till and bedrock mineralogy in the province of Småland, southern Sweden. Geoderma 136, 643-659.

Alapieti, T., 1982. The Koillismaa layered igneous complex, Finland: its structure, mineralogy and geochemistry, with emphasis on the distribution of chromium. Bull. Geol. Surv. Finl. 319, 116.

Allen, C., Darmody, R., Thorn, C., Dixon, J., Schlyter, P., 2001. Clay mineralogy, chemical weathering and landscape evolution in Arctic-Alpine Sweden. Geoderma 99, 277-294.

Amelin, Y., Semenov, V., 1990. On the age and sources of magmas for the early Proterozoic layered intrusions of Karelia (abstracts of contributions). Isotopic dating of endogenic ore associations, Tbilisi, 40-42.

Amelin, Y.V., Semenov, V.S., 1990. Age and magma source of the early Paleoproterozoic layered intrusions of Karelia (in Russian). In Proceedings of all-USSR conference "Isotope dating of endogenous ore formations", XXIV session, Tbilisi, November 12-18, 1990, 40-42.Amelin, Y.V., Heaman, L., Semenov, V., 1995. U-Pb geochronology of layered mafic intrusions in the eastern Baltic Shield: implications for the timing and duration of Paleoproterozoic continental rifting. Precambrian Res. 75, 31-46.

Amelin, Y.V., Semenov, V.S., 1996. Nd and Sr isotopic geochemistry of mafic layered intrusions in the eastern Baltic shield: implications for the evolution of Paleoproterozoic continental mafic magmas. Contrib. Mineral. Petrol. 124, 255-272.

Ameijeiras-Marino, Y., Opfergelt, S., Schoonejans, J., Vanacker, V., Sonnet, P., de Jong, J., Delmelle, P., 2017. Impact of low denudation rates on soil chemical weathering intensity: A multiproxy approach. Chem. Geol. 456, 72-84.

Anderson, H., Berrow, M., Farmer, V., Hepburn, A., Russell, J., Walker, A., 1982. A reassessment of podzol formation processes. J. Soil Sci. 33, 125-136.

Andersson, P. S., Porcelli, D., Gustafsson, O., Ingri, J., Wasserburg, G. J., 2001. The importance of colloids for the behavior of uranium isotopes in the low-salinity zone of

844 a stable estuary. Geochim. Cosmochim. Acta 65(1), 13–25.
845 Andersson, K., Dahlqvist, R., Turner, D., Stolpe, B., Larsson, T., Ingri, J., Andersson, P.,
846 2006. Colloidal rare earth elements in a boreal river: Changing sources and
847 distributions during the spring flood. Geochim. Cosmochim. Acta 70, 3261-3274.
848 Andrews, L.C., Catania, G.A., Hoffman, M.J., Gulley, J.D., Lüthi, M.P., Ryser, C., Hawley,
849 R.L., Neumann, T.A., 2014. Direct observations of evolving subglacial drainage
850 beneath the Greenland Ice Sheet. Nature 514, 80-83.
851 Bagard M.-L., Schmitt A.-D., Chabaux F., Pokrovsky O.S., Viers J., Stille P., Labolle F.,
852 Prokushkin A.S. (2013) Biogeochemistry of stable Ca and radiogenic Sr isotopes in
853 larch-covered permafrost-dominated watersheds of Central Siberia. Geochimica
854 Cosmochimica Acta, 114, 169–187.
855 Balagizi, C., Darchambeau, F., Bouillon, S., Yalire, M., Lambert, T., Borges, A., 2015. River
856 geochemistry, chemical weathering, and atmospheric CO2 consumption rates in the
857 Virunga Volcanic Province (East Africa). G^3, 16, 2637-2660.
858 Balashov, Y.A., Bayanova, T.B., Mitrofanov, F. P., 1993. Isotope data on the age and genesis
859 of layered basic-ultrabasic intrusions in the Kola Peninsula and northern Karelia,
860 northeastern Baltic Shield. Precambrian Res. 64, 197-205.
861 Barkov, A., Gannibal, L., Ryungenen, G., Balashov, Y., 1991. Zircon dating of the Kivakka
862 layeres massif, Northern Karelia. Abstracts of papers. All-USSR seminar on methods
863 of isotopic geology, Zvenigorod, 21-25 October 1991, St. Petersburg, 21-23.
864 Bau, M., 1999. Scavenging of dissolved yttrium and rare earths by precipitating iron
865 oxyhydroxide: Experimental evidence for Ce oxidation, Y-Ho fractionation, and
866 lanthanide tetrad effect. Geochim. Cosmochim. Acta 63, 67-77.
867 Berner, R. A., Lasaga, A. C., Garrels, R. M., 1983. The carbonate-silicate geochemical cycle
868 and its effect on atmospheric carbon dioxide over the past 100 million years. Am. J.
869 Sci. 283, 641-683.
870 Berner, R., 1992. Weathering, plants, and the long-term carbon cycle. Geochim. Cosmochim.
871 Acta 56(8), 3225-3231.
872 Berner, R., 1995. Chemical weathering and its effect on atmospheric CO_2 and climate.
873 Reviews in Mineralogy and Geochemistry 31(1), 565-583.
874 Berner, R., Caldeira, K., 1997. The need for mass balance and feedback in the geochemical
875 carbon cycle. Geology 25, 955-956. Bibikova, E. V., Samsonov, A. V., Petrova, A. Y.,
876 Kirnozova, T. I., 2005. The Archean geochronology of Western Karelia. Stratigraphy
877 and Geological Correlation 13(5), 459-475.
878 Boeglin, J., Probst, J., 1998. Physical and chemical weathering rates and CO_2 consumption in
879 a tropical lateritic environment: the upper Niger basin. Chem. Geol. 148(3-4), 137-
880 156.
881 Brady, P.V., 1991. The Effect of silicate weathering on global temperature and atmospheric
882 CO_2. Journal of Geophysical Research 96(B11), 18101-18106.
883 Breemen van, N., Buurman, P., 1998. Soil Formation, 245-270. Kluwer Academic Publishers,
884 Dordrecht, Boston.
885 Brimhall, G. H., Lewis, C. J., Ford, C., Bratt, J., Taylor, G., Warin, O., 1991. Quantitative
886 geochemical approach to pedogenesis: importance of parent material reduction,
887 volumetric expansion, and eolian influx in lateritization. Geoderma 51, 51-91.
888 Buurman, P., 1984. Podzols: Temperate regions (Van Nostand Reinhold soil science series).
889 Van Nostand Reinhold , New York. Buurman, P., Jongmans, A., 2005. Podzolisation
890 and soil organic matter dynamics. Geoderma 125(1-2), 71-83.
891 Bychkova, Y.V., 2003. Structural patterns of contrasting rhythmic layering of Kivakka
892 intrusion. PhD thesis, Moscow State University.
893 Bychkova, Y., Koptev-Dvornikov, E., 2004. Rhytmical layering of Kivakka type: geology,

petrology, petrochemistry, hypothesis of formation (in Russian). Petrology 12(3), 281-302.
Bychkova, Y. V., Koptev-Dvornikov, E. V., Kononkova, N. N., Kameneva, E. E., 2007. Composition of rock-forming minerals in the Kivakka layered massif, Northern Karelia, and systematic variations in the chemistries of minerals in the rhythmic layering subzone. Geochemistry International 45(2), 131–151.
Caritat de, P., Reimann, C., Bogatyrev, I., Chekushin, V., Finne, T. E., Halleraker, J. H., Kashulina, G., Niskavaara, H., Pavlov, V., Ayras, M., 2001. Regional distribution of Al, B, Ba, Ca, K, La, Mg, Mn, Na, P, Rb, Si, Sr, Th, U and Y in terrestrial moss within a 188,000 km^2 area of the central Barents region: infuence of geology, seaspray and human activity. Appl. Geochem. 16, 137-159.
Condie, K. C., 1993. Chemical composition and evolution of the upper continental crust: Contrasting results from surface samples and shales. Chem. Geol. 104(1-4), 1-37.
Cornu, S., Lucas, Y., Lebon, E., Ambrosi, J. P., Luizão, F., Rouiller, J., Bonnay, M., Neal, C., 1999. Evidence of titanium mobility in soil profiles, Manaus, central Amazonia. Geoderma 91(3-4), 281-295.
Courchesne, F., Hendershot, W., 1997. Essai. La Genèse des podzols', Geogr. Phys. Quarter. 51, 235-250.
Dahlqvist, R., Benedetti, M. F., Andersson, K., Turner, D., Larsson, T., Stolpe, B., Ingri, J., 2004. Association of calcium with colloidal particles and speciation of calcium in the Kalix and Amazon rivers. Geochim. Cosmochim. Acta 68(20), 4059-4075.
Dahlqvist, R., Andersson, K., Ingri, J., Larsson, T., Stolpe, B., Turner, D., 2007. Temporal variations of colloidal carrier phases and associated trace elements in a boreal river. Geochim. Cosmochim. Acta 71, 5339-5354.
D'Amico, M., Julitta, F., Previtali, F., Cantelli, D., 2008. Podzolization over ophiolitic materials in the western Alps (Natural Park of Mont Avic, Aosta Valley, Italy). Geoderma 146, 129-137.
Debon, F., Enrique, P., Autran, A., 1995. Magmatisme Hercynien. Synthèse géologique et géophysique des Pyrenees. Edt BRGM 1, Cycle Hercynien (eds. A. Barnolas and J. C. Chiron), 361-499.
DePaolo, D., Wasserburg, G., 1976. Inferences about magma sources and mantle structure from variations of $^{143}Nd/^{144}Nd$. Geophys. Res. Lett. 3, 249-252.
DePaolo, D. J., 1981. Neodymium isotopes in the Colorado Front Range and crust-mantle evolution in the Proterozoic. Nature 291, 193-196.
DePaolo, D., 1988. Neodymium isotope geochemistry: an introduction. Springer-Verlag, New York, p. 187.
Dessert, C., Dupré, B., Francois, L. M., Schott, J., Gaillardet, J., Chakrapani, G., Bajpai, S., 2001. Erosion of Deccan Traps determined by river geochemistry: impact on the global climate and the $^{87}Sr/^{86}Sr$ ratio of seawater. Earth Planet. Sci. Lett. 188, 459-474.
Dessert, C., Dupré, B., Gaillardet, J., François, L. M., Allègre, C. J., 2003. Basalt weathering laws and the impact of basalt weathering on the global carbon cycle. Chem. Geol. 202, 257-273.
Dessert, C., Lajeunesse, E., Lloret, E., Clergue, C., Crispi, O., Gorge, C., Quidelleur, X., 2015. Controls on chemical weathering on a mountainous volcanic tropical island: Guadeloupe (French West Indies). Geochimica et Cosmochimica Acta 171, Pages 216-237.Deuerling, K.M., Martin, J.B., Martin, E.E., Scribner, C.A., 2018. Hydrologic exchange and chemical weathering in a proglacial watershed near Kangerlussuaq, west Greenland. J. Hydrol. 556, 220-232.
Dokuchaev, V., 1880. On podzol (in Russian). Trudy Volnogo ekonomicheskogo obschestva 1(2), 142-150.

Dupré, B., Gaillardet, J., Rousseau, D., Allègre, C. J., 1996. Major and trace elements of river-borne material: The Congo Basin. Geochim. Cosmochim. Acta 60(8), 1301-1321.

Dupré, B., Dessert, C., Oliva, P., Godderis, Y., Viers, J., Francois, L., Millot, R., Gaillardet, J., 2003. Rivers, chemical weathering and Earth's climate. C. R. Geoscience 335, 1141-1160.

Eiriksdottir, E., Gislason, S., and Oelkers, E., 2013. Does temperature or runoff control the feedback between chemical denudation and climate? Insights from NE Iceland: Geochimica et Cosmochimica Acta, v. 107, p. 65–81

Eiriksdottir, E.S., Gislason, S.R., Oelkers, E.H., 2015. Direct evidence of the feedback between climate and nutrient, major, and trace element transport to the oceans. Geochim. Cosmochim. Acta 166, 249-266.

Erlandsson, M., Oelkers, E.H., Bishop, K., Sverdrup, H., Belyazid, S., Ledesma, J.L.J., Köhler, S.J., 2016. Spatial and temporal variations of base cation release from chemical weathering on a hillslope scale. Chemical Geol. 441, 1-13.

Fedo, C. M., Nesbitt, H. W., Young, G. M., 1995. Unraveling the effects of potassium metasomatism in sedimentary rocks and paleosols, with implications for paleoweathering conditions and provenance. Geology 23(10), 921-924.

Feoktistov, V. M., 2004. Water chemical composition of Karelian rivers and their dissolved chemical discharge into the White Sea. Water Resour. 31(6), 631-638.

Ferrier, K. L., Riebe, C. S., Hahm, W. J., 2016. Testing for supply-limited and kinetic-limited chemical erosion in field measurements of regolith production and chemical depletion, Geochem. Geophys. Geosyst. 17, 2270–2285.

Foster, G.L., Vance, D., 2006. Negligibe glacial-interglacial variation in continental chemical weathering rates. Nature 444, 918-921.

Gaillardet, J., Dupré, B., Louvat, P., Allègre, C., 1999. Global silicate weathering and CO_2 consumption rates deduced from the chemistry of large rivers. Chem. Geol. 159, 3-30.

Gaillardet, J., Rad, S., Rive, K., Louvat, P., Gorge, C., Allègre, C.J., Lajeunesse, E., 2011. Orography-driven chemical denudation in the Lesser Antilles: Evidence for a new feed-back mechanism stabilizing atmospheric CO_2. American Journal of Science 311, 851-894.Giesler, R., Ilvesniemi, H., Nyberg, L., van Hees, P., Starr, M., Bishop, K., Kareinen, T., Lundström, U., 2000. Distribution and mobilization of Al, Fe and Si in three podzolic soil profiles in relation to the humus layer. Geoderma 94, 249-263.

Gislason, S. R., Arnorsson, S., Armannsson, H., 1996. Chemical weathering of basalt in Southwest Iceland, effects of runoff, age of rocks and vegetative/glacial cover. American Journal of Science 296, 837-907.

Goldstein, S., O'Nions, R., Hamilton, P. 1984. A Sm-Nd study of atmospheric dusts and particulates from major river system. Earth Planet. Sci. Lett. 70, 221-236.

Grard, A., François, L., Dessert, C., Dupré, B., Goddéris, Y., 2005. Basaltic volcanism and mass extinction at the Permo-Triassic boundary: Environmental impact and modeling of the global carbon cycle. Earth Planet. Sci. Lett. 234(1-2), 207-221.

Hättestrand, C. (1997), Ribbed moraines in Sweden – distribution pattern and palaeoglaciological implications, Sedimentary Geology 111, 41-56.

Hawley, S.M., Pogge von Strandmann, P.A.E., Burton, K.W., Williams, H.M., Gislason, S.R., 2017. Continental weathering and terrestrial (oxyhydr)oxide export: Comparing glaial and non-glacial catchments in Iceland. Chem. Geol. 462, 55-66.

Hindshaw, R.S., Rickli, J.R., Leuthold, J., Wadham, J., Bourdon, B., 2014. Identifying weathering sources and processes in an outlet glacier oft he Greenland Ice Sheet using Ca and Sr isotope ratios. Geochim. Cosmochim. Acta 145, 50-71.

Horton, T., Chamberlain, C.P., Fantle, M., Blum, J., 1999. Chemical weathering and

994 lithologic controls of water chemistry in a high-elevation river system: Clark's Fork of
995 the Yellowstone river, Wyoming and Montana. Water Resour. Res., 35, 1643-1655.
996 Ibarra, D., Caves, J., Moon, S., Thomas, D., Hartmann, J., Page Chamberlain, C., Maher, K.,
997 2016. Differential weathering of basaltic and granitic catchments from concentration–
998 discharge relationships. Geochimica et Cosmochimica Acta 190, 265-293.
999 Ingri, J., Widerlund, A., Land, M., Gustafsson, O., Andersson, P. S., Öhlander, B., 2000.
1000 Temporal variations in the fractionation of the rare earth elements in a boreal river, the
1001 role of colloidal particles. Chem. Geol. 166, 23-45.
1002 Ingri, J., Widerlund, A., Land, M., 2005. Geochemistry of major elements in a pristine boreal
1003 river system, hydrological compartments and flow paths. Aquatic Geochemistry 11,
1004 57-88.
1005 Jacobsen, S. B., Wasserburg, G., 1980. Sm-Nd isotopic evolution of chondrites. Earth Planet.
1006 Sci. Lett. 50(1), 139-155.
1007 Kempton, P. D., Downes, H., Neymark, L. A., Wartho, J. A., Zartman, R. E., Sharkov, E. V.,
1008 2001. Garnet granulite xenoliths from the northern Baltic Shield – the underplated
1009 lower crust of a palaeoproterozoic large igneous province? J. Petrol. 42(4), 731-763.
1010 Klyunin, S., Grokhovskaya, T., Zakharov, A., Solovjeva, T., 1994. Geology and platinum-
1011 bearing potential of the Olanga group of massifs, Northern Karelia (in Russian).
1012 Geologiya i genesis mestorozhdenii platinovykh metallov. Nauka, Moscow, 111-126.
1013 Koptev-Dvornikov, E. V., 2001. Distribution of cumulative mineral assemblages, major and
1014 trace elements over the vertical c of the Kivakka intrusion, Olanga group of intrusions,
1015 Northern Karelia. Petrology 9(1), 3-27.
1016 Kulikov, V., Kulikova, V., 1982. On the summary section of the early Precambrian of the
1017 Vetreny belt (in Russian). Geology and Stratigraphy of Karelian Precambrian Rocks.
1018 Petrozavodsk, Year Book Information, 21-26.
1019 Kulikov, V., 1999. Komatiitic Basalts of the Vetreny Belt (in Russian). Selected Works of the
1020 Karelian Scientific Center of Russian Academy of Sciences, 60-61.
1021 Kulikov, V., Kulikova, V., Bychkova, Y., Zudin, A., 2003. Sumian rifting volcanism of
1022 Paleoproterozoi in South-Eastern part of Karelian Kraton. Proceedings of the II All-
1023 Russian symposium on volcanology and paleovolcanology "Vulkanizm i
1024 geodinamika". Ekaterinburg, 99-104.
1025 Kulikov, V., Bychkova, Y., Kulikova, V., Koptev-Dvornikov, E., Zudin, A., 2005. Role of
1026 deep-seated differentiation in formation of Paleoproterozoic Sinegorie lava plateau of
1027 komatiite basalts, southeastern Fennoscandia. Petrology 13(5), 469-488.
1028 Kulikova, V.V., Kulikov, V.S., 1981. New data on Archean peridotitic komatiites in East
1029 Karelia. Dokl. Akad. Nauk SSSR. 259(3), 693-697.
1030 Kump, L. R., Brantley, S. L., Arthur, M. A., 2000. Chemical weathering, atmospheric CO_2,
1031 and climate. Annu. Rev. Earth Planet. Sci. Lett. 28, 611-667.
1032 Land, M., Ingri, J., Öhlander, B., 1999a. Past and present weathering rates in northern
1033 Sweden. Appl. Geochem. 14, 761-774.
1034 Land, M., Öhlander, B., Ingri, J., Thunberg, J., 1999b. Solid speciation and fractionation of
1035 rare earth elements in a spodosol profile from northern Sweden as revealed by
1036 sequential extraction. Chem. Geol. 160, 121-138.
1037 Land, M., Ingri, J., Andersson, P. S., Öhlander, B., 2000. Ba/Sr, Ca/Sr and $^{87}Sr/^{86}Sr$ ratios in
1038 soil water and groundwater: implications for relative contributions to stream water
1039 discharge. Appl. Geochem. 15, 311-325.
1040 Land, M., Öhlander, B., 2000. Chemical weathering rates, erosion rates and mobility of major
1041 and trace elements in a boreal granitic till. Aquat. Geochem. 6, 435-460.
1042 Land, M., Thunberg, J., Öhlander, B., 2002. Trace metal occurrence in a mineralised and a
1043 non-mineralised spodosol in northern Sweden. J. Geochem. Explor. 75, 71-91.

1044 Lavrov, M., 1979. Ultramafic and layered peridotite-gabbro-norite intrusions in Precambrian
1045 in Northern Karelia. Nauka, Leningrad, 135 p.
1046 Lesovaya, S., Goryachkin, S., Pogozhev, E., Polekhovskii, Y., Zavarzin, A., Zavarzina, A.,
1047 2008. Soils on hard rocks in the Northwest of Russia: Chemical and mineralogical
1048 properties, genesis, and classification problems. Eurasian Soil Science 41(4), 363-376.
1049 Lesovaya, S., GoryachkinYu, S.V., Polekhovskii, S., 2012. Soil formation and weathering on
1050 ultramafic rocks in the mountainous tundra of the Rai-Iz massif, Polar Urals. Eurasian
1051 Soil Science Volume 45, Issue 1, pp 33–44.
1052 Li, C., Yang, S., 2010. Is chemical inex of alteration (CIA) a reliable proxy for chemical
1053 weathering in global drainage basin? Am. J. Sci. 310, 111-127.
1054 Lobach-Zhuchenko, S., Levchenkov, O., Cherulaev, V., Krylov, I., 1986. Geological
1055 evolution of the Karelian granite-greenstone terrain. Precambrian Res. 33(1-3), 45-65.
1056 Lobach-Zhuchenko, S., Chekulayev, V., Sergeev, S., Levchenkov, O., Krylov, I., 1993.
1057 Archaean rocks from southeastern Karelia (Karelian granite greenstone terrain).
1058 Precambrian Res. 62(4), 375-397.
1059 Lobach-Zhuchenko, S., Arestova, N., Chekulaev, V., Levsky, L., Bogomolov, E., Krylov, I.,
1060 1998. Geochemistry and petrology of 2.40-2.45 Ga magmatic rocks in the north-
1061 western Belomorian Belt, Fennoscandian Shield, Russia. Precambrian Res. 92, 223-
1062 250.
1063 Louvat, P., Allègre, C. J., 1997. Present denudation rates on the island of Réunion determined
1064 by river geochemistry: Basalt weathering and mass budget between chemical and
1065 mechanical erosions. Geochim. Cosmochim. Acta 61(17), 3645-3669.
1066 Louvat, P., Allègre, C. J., 1998. Riverine erosion rates on Sao Miguel volcanic island, Azores
1067 archipelago. Chem. Geol. 148(3-4), 177-200.
1068 Lozovik, P., Potapova, I., 2006. Input of chemical substances with atmospheric precipitation
1069 onto the territory of Karelia. Water Resour. 33(1), 104-111.
1070 Lundström, U., 1993. The role of organic acids in soil solution chemistry in a podzolized soil.
1071 J. Soil Sci. 44, 121-133.
1072 Lundström, U. S., van Breemen, N., Bain, D., 2000a. The podzolization process. A review.
1073 Geoderma 94, 91-107.
1074 Lundström, U. S., van Breemen, N., Bain, D. et al., 2000b. Advances in understanding the
1075 podzolization process resulting from a multidisciplinary study of three coniferous
1076 forest soils in the Nordic Countries. Geoderma 94(2-4), 335-353.
1077 Maher, K., 2011. The role of fluid residence time and topographic scales in determining
1078 chemical fluxes from landscapes. Earth Planet. Sci. Lett., 312, 48-58.
1079 Maher, K., Chamberlain, C.P., 2014. Hydrologic regulation of chemical weathering and the
1080 geologic. Science, 343, 1502-1504.
1081 Maksimova, M., 1967. Inorganic and organic composition of major ions in rivers of Karelian
1082 coast of the White Sea (in Russian). Gidrobiologicheskie issledovaniya na Karelskom
1083 poberezhie Belogo morya. Nauka, Leningrad, 9-20.
1084 Melkerud, P., Bain, D., Jongmans, A., Tarvainen, T., 2000. Chemical, mineralogical and
1085 morphological characterization of three podzols developed on glacial deposits in
1086 Northern Europe. Geoderma 94, 125-148.
1087 Meunier, A., Caner, L., Hubert, F., El Alabani, A., Prêt D., 2013. The weathering intensity
1088 scale (WIS) : an alternative approach of the chemical index of alteration. American
1089 Journal of Science,Vol.313, 113–143.
1090 Millot, R., Gaillardet, J., Dupré, B., Allègre, C.J., 2002. The global control of silicate
1091 weathering rates and the coupling with physical erosion: new insights from rivers of
1092 the Canadian Shield. Earth Planet. Sci. Lett. 196, 83–98.
1093 Millot, R., Gaillardet, J., Dupré, B., Allègre, C. J., 2003. Northern latitude chemical

1094 weathering rates: Clues from the Mackenzie River basin, Canada. Geochim.
1095 Cosmochim. Acta 67(7), 1305-1329.
1096 Mokma, D., Yli-Halla, M., Lindqvist, K., 2004. Podzol formation in sandy soils of Finland.
1097 Geoderma 120, 259-272.
1098 Muir, A., 1961. The podzol and podzolic soils. Advances in Agronomy 13, 1-56.
1099 Murashkina, M., Southard, R., Pettygrove, G., 2007. Silt and fine sand fractions dominate K
1100 fixation in soils derived from granitic alluvium of the San Joaquin Valley, California.
1101 Geoderma 141, 283-293.
1102 Nesbitt, H. W., Young, G. M., 1982. Early Proterozoic climates and plate motions inferred
1103 from major element chemistry of lutites. Nature 299, 715-717.
1104 Öhlander, B., Ingri, J., Ponter, C., 1991. Geochemistry of till weathering in the Kalix River
1105 Watershed, northern Sweden. Reports in forest ecology and forest soils, Swedish
1106 University of Agricultural Sciences. In: Chemical weathering under field conditions
1107 (ed. K. Rosén) 63, 1-18.
1108 Öhlander, B., Land, M., Ingri, J., Widerlund, A., 1996. Mobility of rare earth elements during
1109 weathering of till in northern Sweden. Appl. Geochem. 11, 93-99.
1110 Öhlander, B., Thunberg, J., Land, M., Hoglund, L. O., Quishang, H., 2003. Redistribution of
1111 trace metals in a mineralized spodosol due to weathering, Liikavaara, northern
1112 Sweden. Appl. Geochem. 18, 883-899.
1113 Oliva, P., Viers, J., Dupré, B., Fortune, J. P., Martin, F., Braun, J.-J., Nahon, D., Robain, H.,
1114 1999. The effect of organic matter on chemical weathering: Study of a small tropical
1115 watershed: Nsimi-Zoétélé site, Cameroon. Geochim. Cosmochim. Acta 63(23/24),
1116 4013-4035.
1117 Oliva, P., Dupré, B., Martin, F., Viers, J., 2004. The role of trace minerals in chemical
1118 weathering in a high-elevation granitic watershed (Estibère, France): Chemical and
1119 mineralogical evidence. Geochim. Cosmochim. Acta 68(10), 2223-2244.
1120 Olsson, M. T., Melkerud, P., 2000. Weathering in three podzolized pedons on glacial deposits
1121 in northern Sweden and central Finland. Geoderma 94, 149-161.
1122 Opfergelt, S., Burton, K.W., Georg, R.B., West, A.J., Guicharnaud, R.A., Sigfusson, B.,
1123 Siebert, C., Gislason, S.R., Halliday, A.N., 2014. Magnesium retention on the soil
1124 exchange complex controlling Mg isotope variations in soils, soil solutions and
1125 vegetation in volcanic soils, Iceland. Geochim. Cosmochim. Acta 125, 110-130.
1126 Parry, S.A., Hodson, M.E., Kemp, S.J., Oelkers , E.H., 2015. The surface area and reactivity
1127 of granitic soils: I. Dissolution rates of primary minerals as a function of depth and age
1128 deduced from field observations. Geoderma 237-238, 21-35.
1129 Peuraniemi, V., Aario, R., Pulkkinen, P., 1997. Mineralogy and geochemistry of the clay
1130 fraction of till in northern Finland. Sedimentary Geology 111, 313-327.
1131 Pokrovsky, O.S., Schott, J., 2002. Iron colloids/organic matter associated transport of major
1132 and trace elements in small boreal rivers and their estuaries (NW Russia). Chem. Geol.
1133 190, 141-179.
1134 Pokrovsky, O.S., Schott, J., Kudryavtsev, D. I., Dupré, B., 2005. Basalt weathering in Central
1135 Siberia under permafrost conditions. Geochim. Cosmochim. Acta 69(24), 5659-5680.
1136 Pokrovsky, O. S., Schott, J., Dupré, B., 2006a. Trace element fractionation and transport in
1137 boreal rivers and soil porewaters of permafrost-dominated basaltic terrain in Central
1138 Siberia. Geochim. Cosmochim. Acta 70, 3239-3260.
1139 Pokrovsky, O.S., Schott, J., Dupré, B., 2006b. Basalt weathering and trace elements migration
1140 in the boreal Arctic zone. J. Geochem. Explor. 88, 304-307.
1141 Ponomareva, V., 1964. Theory of podzol-formation process (in Russian). M.-L.: Nauka, p.
1142 380.
1143 Puchtel, I., Hofmann, A., Mezger, K., Shchipansky, A., Kulikov, V., Kulikova, V., 1996.

Petrology of a 2.41 Ga remarkably fresh komatiitic basalt lava lake in Lion Hills, central Vetreny Belt, Baltic Shield. Contrib. Mineral. Petrol. 124(3-4), 273-290.
Puchtel, I. S., Haase, K. M., Hofmann, A. W., Chauvel, C., Kulikov, V. S., Garbe-Schonberg, C., Nemchin, A. A., 1997. Petrology and geochemistry of crustally contaminated komatiitic basalts from the Vetreny Belt, southeastern Baltic Shield: Evidence for an early Proterozoic mantle plume beneath rifted Archean continental lithosphere. Geochim. Cosmochim. Acta 61(6), 1205-1222.
Raymon, P.A., 2017. Temperature versus hydrological controls of chemical weathering fluxes from United States forests. Chem. Geol. 458, 1-13.
Reimann, C., Melezhik, V., 2001. Metallogenic provinces, geochemical provinces and regional geology - what causes large-scale patterns in low density geochemical maps of the C-horizon of podzols in Arctic Europe? Appl. Geochem. 16(7-8), 963-983.
Remaury, M., Oliva, P., Guillet, B., Martin, F., Toutain, F., Dagnac, J., Belet, J., Dupré, B., Gauquelin, T., 2002. Nature and genesis of spodic horizons characterized by inverted color and organic content in a subalpine podzolic soil (Pyrenees Mountains, France). Bulletin de la Société Géologique de France 172(1), 77-86.
Revyako, N., Bychkova, Y., Kostitsyn, Y., 2007. Isotope evidence of the interaction of basic melt with crust rocks on the example of Kivakka layered intrusion (Karelia) (in Russian). Proccedings of International conference "Ultrabasic-basic complexes of fold regions". Irkutsk, 487-490.
Riebe, C. S., Kirchner, J. W., Granger, D. E., Finkel, R. C., 2001 Strong tectonic and weak climatic control of long-term chemical weathering rates. Geology 29, 511-514.
Riebe, C. S., Kirchner, J. W., Finkel, R. C., 2004. Erosional and climatic effects on long-term chemical weathering rates in granitic landscapes spanning diverse climate regimes. Earth Planet. Sci. Letters 224, 547-562.
Righi, D., Chauvel, A., 1987. Podzols and Podzolization. Assoc. Franc. Etude Sol. INRA, Plaisir et Paris, Paris.
Ryabchikov, I., Suddaby, P., Girnis, A., Kulikov, V., Kulikova, V., Bogatikov, O., 1988. Trace-element geochemistry of Archaean and Proterozoic rocks from eastern Karelia, USSR. Lithos 21, 183-194.
Salminen, R., Gregorauskiene, V., Tarvainen, T., 2008. The normative mineralogy of 10 soil profiles in Fennoscandia and north-western Russia. Appl. Geochem. 23(12), 3651-3665.
Sarala, P., 2005. Till geochemistry in the ribbed moraine area of Peräpohjola, Finland. Appl. Geochem. 20, 1714-1736.
Sawhney, B.L., 1989. Minerals in soil environments. Soil Science Society of America, chapter 16: Interstratification in layer silicates, 789-828.
Schopka, H., Derry, L., Arcilla, C., 2011. Chemical weathering, river geochemistry and atmospheric carbon fluxes from volcanic and ultramafic regions on Luzon Island, the Philippines. Geochim. Cosmochim. Acta 75, 978-1002.Schopka, H., Derry, L., 2012. Chemical weathering fluxes from volcanic islands and the importance of groundwater: The Hawaiian example. Earth and Planetary Science Letters 339-340, 67–78.
Schroeder, P.A., Melear, N.D., West, L.T., Hamilton, D.A., 2000. Meta-gabbro weathering in the Georgia Piedmont, USA: implications for global silicate weathering rates. Chem. Geol. 163, 235-245.
Schweda, P., Araujo, P. D. R., Sjoeberg, L., 1991. Soil chemistry, clay mineralogy and noncrystalline phases in soil profiles from southern Sweden and Gårdsjön.. In: Rosén, K. (Ed.), Chemical weathering under field conditions. Reports in Forest Ecology and Forest Soils. Swedish University of Agricultural Sciences 63, 49-62.
Semenov, V., Koptev-Dvornikov, E., Berkovskii, A., Kireev, B., Pchelintseva, N., Vasil'eva,

M., 1995. Layered troctolite-gabbro-norite Tsipinga intrusion, Northern Karelia: Geologic structure and petrology. Petrology 3(6), 588-610.
Shmygalev, V., 1968. Mafic and ultramafic intrusions of the Olanga group. Proterozoic volcanic and ultramafic complexes of Karelia 1, 209-219.
Simonsson, M., Bergholm, J., Olsson, B.A., von Brömssen, C., Öborn, I., 2015. Estimating weathering rates using base cation budgets in a Norway spruce stand on podzolised soil: Analysis of fluxes and uncertainties. Forest Ecol. Management, 340, 135-152.
Starr, M., Lindroos, A., Ukonmaanaho, L., Tarvainen, T., Tanskanen, H., 2003. Weathering release of heavy metals from soil in comparison to deposition, litterfall and leaching fluxes in a remote, boreal coniferous forest. Appl. Geochem. 18, 607-613.
State Geological Map of Russian Federation, 2001. In: Bogdanov, Yu.B. (Ed.), Explication Note. Ministery of Natural Ressources, St-Petersbourg, VSEGEI. Sheet Q-(35)-37.
Sun, X., Mörth, C.-M., Humbord, C., Gustafsson, B., 2017. Temporal and spatial variations of rock weathering and CO_2 consumption in the Baltic Sea catchment. Chem. Geol. 466, 57-69.
Stroeven, A.P., Hättestrand, C., Kleman, J., Heyman, J., Fabel, D., Fredin, O., Goodfellow, B.W., Harbor, J.M., Jansen, J.D., Olsen, L., 2016. Deglaciation of Fennoscandia. Quaternary Sci. Rev. 147, 91-121.
Taylor, S., McLennan, S., 1985. The continental crust: its composition and evolution. Blackwell Scientific Publications, Oxford, p. 312.
Thiede, J., Bauch, H. A., Hjort, C., Mangerud, J., 2001. The late Quaternary stratigraphy and environments of northern Eurasia and the adjacent Arctic seas - new contributions from QUEEN. Global and Planetary Change 31(1-4), vii-x.
Thorn, C.E., Dixon, J.C., Darmody, R.G., Allen, C.E., 2006. A 10-year record of the weathering rates of surficial pebbles in Kärkevagge, Swedish Lapland. Catena 65, 272-278.
Tyler, G., 2004. Vertical distribution of major, minor, and rare elements in a Haplic Podzol. Geoderma 119, 277-290.
Vasiliev, M.V., 2006. Specific features of Vetreny Belt paleorift intrusive systems (in Russian). M.Sc. thesis, Faculty of Geology, Moscow State University.
Vasyukova, E., Pokrovsky, O.S., Viers, J., Oliva, P., Dupré, B., Martin, F., Candaudap, F., 2010. Trace elements in organic- and iron-rich surficial fluids of boreal zone: Assessing colloidal forms via dialysis and ultrafiltration. Geochim. Cosmochim. Acta 74, 449-468.
Viers, J., Dupré, B., Braun, J., Deberdt, S., Angeletti, B., Ngoupayou, J. N., Michard, A., 2000. Major and trace element abundances, and strontium isotopes in the Nyong basin rivers (Cameroon): constraints on chemical weathering processes and elements transport mechanisms in humid tropical environments. Chem. Geol. 169, 211-241.
Wymore, A.S., Brereton, R.L., Ibarra, D.E., Maher, K., McDOwell, W.H., 2017. Critical zone structure controls concentration-discharge relationships and solute generation in forested tropical montane watersheds. Water Resources Res., 53(7), 6279-6295.
World reference base for soil resources (IUSS Working Group WRB, FAO), 2006.
Zakharova, E., Pokrovsky, O. S., Dupré, B., Gaillardet, J., Efimova, L., 2007. Chemical weathering of silicate rocks in Karelia region and Kola peninsula, NW Russia: Assessing the effect of rock composition, wetlands and vegetation. Chem. Geol. 242, 255-277.
Zilliacus, H., 1989. Genesis of De Geer moraines in Finland. Sediment. Geol. 62(2-4), 309-317.

1243 **Table 1.** Soils and surface waters studied and their bedrock composition. Sample series from
1244 Vetreny Belt paleorift and Kivakka intrusion are defined as "V" and "K", respectively.
1245 Samples marked with "w" correspond to surface waters and with "ss" - to soil
1246 solutions.

1247

Sample no.	Description	Bedrock composition
Soils		
V-4	Podzol	Komatiitic basalts, glacial deposits
V-7	Podzol	Komatiitic basalts, glacial deposits
V-9	Regosol	Gneisses, glacial deposits
V-15	Regosol	Peridotites
V-16	Podzol	Gneisses, glacial deposits
K-7	Podzol	Gneisses, glacial deposits
K-8	Podzol	Gneisses, glacial deposits
K-14	Podzol	Olivinite
K-29	Regosol	Gneisses, glacial deposits
K-37	Podzol	Gabbro-norites
Waters		
V-3-w	Surface water	Basalt
V-9-w	r. Ruiga	Basalt
V-10-w	Surface water from basalt field	Basalt
V-11-w	Surface water from basalt field	Basalt
V-12-w	r. Ruiga, upstream biofilms	Basalt
V-13-w	r. Ruiga, highest upstream	Basalt
V-15-w	Creek over ultramafites	Ultramafites
V-18-w	r. Nukhcha	Basalt
K-7-w	r. Palajoki, tributary	Gneisses, glacial deposits
K-8-w	Subsurface flow (right bank of the r. Palajoki)	Gneisses, glacial deposits
K-10-w	Swamp (corresponds to K-43 and K-44)	Gabbro-norites
K-12-w	Spring from a swamp	Gneisses, glacial deposits
K-13-w	River over olivenites	Olivinite
K-17-w	Subsurface flow	Norites
K-30-w	r. Vartalambina downstream	Gneisses, glacial deposits
K-31-w	r. Vartalambina upstream, tributary	Gneisses, glacial deposits
K-32-w	Swamp	Gabbro-norites
K-33-w	Stream	Gabbro-norites
K-38-w	Swamp	Gabbro-norites
K-39-w	Swamp	Gabbro-norites
K-41-w	r. Molodilny (springing from swamp)	Gabbro-norites
K-43-w	Swamp	Gabbro-norites
K-44-w	Swamp	Gabbro-norites
K-45-w	r. Palajoki	Gneisses, glacial deposits
Soil solutions		
V-16-ss	Soil water	Peridotites, olivinites
K-5-ss	Soil solution	Gabbro-norites
K-35-ss	Soil solution	Norites

1248

Table 2. Major, trace elements (μg L^{-1}) and dissolved organic carbon (DOC) concentrations, and strontium isotopic ratios ($^{87}Sr/^{86}Sr$) measured in the dissolved phase (i. e. < 0.22 (0.45) μm) in river and swamp waters from Vetreny Belt (sampled on 12-23 July 2004) and Kivakka intrusion zone (sampled on 10-19 July 2006). "nm" stands for not measured; "<dl" – below detection limit; "TDS" – total dissolved solids; "RW" – river water; "SW" – surface water; "SWW" – mire water; "SS" – soil solution; γ – felsic substratum; β – basaltic substratum; G-n – gabbro-norite; N – norite; Ol – olivinite; P – peridotite.

Vetreny Belt	V-9-w	V-12-w	V-13-w	V-15-w	V-18-w	V-10-w	V-11-w	V-3-w	V-16-sw
0.22 μm	RW	RW	RW	RW	RW	SW	SW	SW	SS
μg/l	β	β	β	P	β	β	β	β	P
pH	5.92	5.9	6.5	5.07	7.05	5.18	5.18	5.46	7.11
t°C	20	27	27	25	23	29	29	23	24
DOC, mg/l	36.5	34.7	35.7	39.7	17.2	8.8	98.5	9.8	20.6
Na^+	2 335	2 532	2 215	1 687	4 430	1 800	2 045	1 365	1 508
K^+	514	469	407	106	224	517	304	305	651
Mg^{2+}	2 867	2 793	6 034	3 128	2 917	425	328	544	8 023
Ca^{2+}	1 838	1 811	1 689	837	2 943	1 296	922	1 112	516
H_4SiO_4	4 900	5 070	4 030	4 020	2 210	3 970	4 540	2 930	5 980
Cl^-	1 270	nm	1 590	2 080	3 900	1 582	2 460	1 350	2 210
SO_4^{2-}	750	nm	531	531	800	900	810	1 540	1 590
NO_3^-	<dl	<dl	480	295	101	100	<dl	290	539
F^-	70	<dl	<dl	39	56	28	<dl	33	<dl
[Alk], mg/l	4.85	5.56	16.6	2.05	28	4.21	4.84	1.77	29.89
Al	nm	537	340	319	56	264	310	244	161
Fe	1 888	865	752	2 374	2 216	618	135	290	311
Rb	0.52	0.59	0.53	0.38	0.48	0.85	0.41	0.56	0.76
Sr	13.00	12.18	11.19	5.08	18.81	11.99	9.24	10.11	4.15
TDS, mg/l	16.4	14.1	18.1	15.4	19.9	11.5	8.6	10.0	21.5
$^{87}Sr/^{86}Sr$	0.723799 ± 20	nm	nm	0.722741 ± 20	0.721984 ± 12	nm	nm	0.715087 ± 17	0.723249 ± 33

Table 2, continued.

Kivakka intrusion	K-7-w	K-8-w	K-12-w	K-30-w	K-31-w	K-45-w	K-13-w	K-17-w	K-33-w
0.45 µm	RW	RW	SW	RW	RW	RW	RW	SW	RW
µg/l	γ	γ	γ	γ	γ	γ	Ol	N	G-n
pH	7.36	5.95	6.56	7.42	7.45	7.31	6.56	6.72	6.13
t°C	16	6	nm	nm	nm	nm	nm	nm	nm
DOC, mg/l	10.42	1.74	5.60	6.32	5.08	94.36	30.55	2.22	6.41
Na^+	1 667	1 379	2 161	2 732	1 714	1 652	1 378	2 044	1 164
K^+	502	315	64	386	907	370	374	72	38
Mg^{2+}	2 106	674	1 451	3 898	7 874	1 821	13 002	1 218	570
Ca^{2+}	9 745	2 047	4 891	10 596	17 435	7 219	1 901	7 385	2 328
H_4SiO_4	3 210	3 990	3 760	4 880	3 290	2 390	7 310	4 560	3 200
Cl^-	568	576	295	393	495	526	453	534	400
SO_4^{2-}	1 498	3 650	2 300	351	688	1 922	432	3 576	736
NO_3^-	<dl	<dl	<dl	<dl	139	<dl	<dl	<dl	<dl
F^-	<dl	<dl	<dl	<dl	<dl	<dl	<dl	<dl	<dl
[Alk], mg/l	27.38	8.28	22.76	39.42	80.20	28.32	40.21	26.17	9.59
Al	26.34	32.30	51.74	7.48	9.76	32.97	191.38	20.07	125.24
Fe	2 589.87	5.59	116.64	115.31	246.79	2 124.46	391.96	3.33	270.26
Rb	1.23	0.99	0.17	0.78	1.79	1.06	1.53	0.20	0.15
Sr	50.89	9.94	12.55	17.20	15.91	36.96	14.26	14.79	8.50
TDS, mg/l	19.30	12.63	14.92	23.24	32.54	15.90	24.85	19.39	8.44
$^{87}Sr/^{86}Sr$	0.721067 ± 15	0.725299 ± 15	0.716615 ± 15	nm	nm	0.721102 ± 12	0.717867 ± 21	0.713467 ± 19	nm

Table 2, continued.

Kivakka intrusion	K-41-w	K-10-w	K-43-w	K-44-w	K-32-w	K-38-w	K-39-w	K-5-ss	K-35-ss
0.45 µm	RW	SWW	SWW	SWW	SWW	SWW	SWW	SS	SS
µg/l	G-n	γ	G-n	G-n	G-n	G-n	G-n	N	G-n
pH	7.17	4.94	5.85	5.41	4.56	4.65	5.03	4.94	nm
t°C	nm	24	16	21	nm	19	nm	6	nm
DOC, mg/l	4.96	29.46	nm	31.59	16.65	11.60	5.28	3.43	40.34
Na^+	1 871	1 031	1 094	1 068	1 399	845	743	569	1 102
K^+	89	58	32	50	190	249	133	77	178
Mg^{2+}	1 068	832	1 327	1 055	384	217	165	114	674
Ca^{2+}	3 166	2 065	3 707	2 382	909	644	674	520	1 305
H_4SiO_4	3 700	1 930	2 780	2 250	2 470	490	760	2 520	4 540
Cl^-	374	725	726	841	1 252	1 180	742	217	1 414
SO_4^{2-}	1 610	494	255	235	332	220	599	1 853	1 868
NO_3^-	<dl	<dl	<dl	<dl	<dl	<dl	<dl	862	595
F^-	<dl	<dl	<dl	<dl	<dl	<dl	<dl	<dl	<dl
[Alk], mg/l	16.61	nm	8.06	2.67	2.20	2.76	2.72	1.77	nm
Al	42.69	453.75	302.11	386.37	163.85	179.22	224.63	274.24	440.35
Fe	36.68	3 876.17	10 507.70	4 778.12	164.02	180.11	237.39	913.91	41.37
Rb	0.17	0.10	0.13	0.08	0.51	0.45	0.24	0.29	0.65
Sr	11.56	12.93	16.71	14.19	4.09	4.02	5.31	3.65	10.44
TDS, mg/l	11.88	11.5	20.7	13.0	7.3	4.2	4.3	7.9	12.2
$^{87}Sr/^{86}Sr$	0.713984 ± 13	nm	0.721347 ± 46	nm	nm	nm	nm	nm	nm

Table 3. Mineralogical composition of studied soils. Number of "+" signs indicates different degree of presence of a mineral in soil, "Tr." stands for "traces". Empty cells correspond to the absence of a mineral in the soil sample.

Mineral composition	Quartz	Feldspar	Amphibole	Illite	Vermiculite	Chlorite	Hydrobiotite	Amorphous phases	Interlayered Mica/Vermiculate	Smectite	Talc
K-7-B	+	++	+	+	++	Tr.					
K-14-B1	Tr.			+	+++	+					
K-14-C			+	+	+++	+					Tr.
K-29-O/A	++	++	+	++		Tr.	++	+	+		
K-29-E	++	++	Tr.	++		Tr.	++	+			
K-37-A	++	++	++	++							
K-37-B1	++	++	+	+	++	+				+	
K-37-B2	++	+	+	+	+	+					
V-16-E	++	++	++	+				++			
V-16-B	++	++	+	+	+			+			
V-4-E	++	+	Tr.	Tr.		+				++	
V-7-B	++	+	+	+	+	++		+			
V-9-A	++	+	+					+			
V-15-O/A			+	+	++					++	

Table 4. Chemical Depletion Fraction (CDF), Chemical Depletion Fraction of individual element (CDFx), Chemical Index of Alteration (CIA), CIA_{soil}/CIA_{rock} ratios and poles (4Si, R^{2+} and M+) calculations for the Weathering Intensity Scale (WIS) diagram. CDF and CDFx were calculated according to Riebe et al. (2004). CIA values were calculated following Nesbitt and Young (1982) considering that all CaO content are coming from silcate phases. WIS poles were established using the reference study of Meunier et al., 2014 by considering monocationic millimoles from oxide amounts : 4Si = mMol Si/4 ; R^{2+} = mMol Mg^{2+} + mMol Mn^{2+} ; M^{+} = mMol Na^{+} + mMol K^{+} + 2xmMol Ca^{2+}. The R2+ component was calculated without considering Fe^{2+} content because only total Fe was measured during chemical analyses.

			Calculated chemical depletion fraction of elements, Ti as invariant										SOIL WIS		
SAMPLE	type of rock	Chemical depletion	% Si	% Al	% Fe	% Ca	% Mg	% Na	% K	% Mn	CIA	CIAsoil/CIArock	% 4Si	% M+	% R2+
soil samples															
K-7 E	γ	51%	0,3	0,6	0,9	0,9	1,0	*-0,1*	*-3,8*	0,9	50	1,01	54,96	41,76	3,27
K-7 B	γ	52%	0,3	0,7	0,7	0,9	0,9	0,0	*-3,0*	0,9	50	1,01	52,57	40,68	6,74
K-8 E	γ	2%	*-0,1*	0,3	0,5	0,7	0,4	0,1	*-0,3*	0,8	50	1,00	56,13	39,22	4,65
K-8 B	γ	*-72%*	*-0,6*	*-0,2*	*-0,6*	0,3	*-0,2*	*-0,3*	*-0,7*	0,6	54	1,08	54,26	39,90	5,84
K-8 C	γ	*-29%*	*-0,4*	0,1	0,2	0,4	*-0,2*	*-0,3*	*-0,6*	0,6	48	*0,98*	52,28	41,45	6,26
K-14 B1	Ol	63%	0,6	0,6	0,6	0,7	0,7	0,6	0,6	0,6	46	1,17	14,87	6,25	78,88
K-14 B2	Ol	81%	0,7	0,2	1,0	0,8	1,0	*-1,0*	*-1,5*	1,0	48	1,21	50,93	37,13	11,94
K-14 C	Ol	32%	0,3	0,4	0,3	0,4	0,3	0,7	0,9	0,3	42	1,06	13,91	5,14	80,95
K-29 O/A	γ	*-520%*	*-0,5*	*-0,3*	0,2	*-0,1*	0,2	*-0,9*	0,5	0,6	45	*0,91*	46,39	50,59	3,01
K-29 C	γ	*-48%*	*-0,6*	*-0,3*	0,5	*-0,1*	0,6	*-0,9*	0,6	0,7	49	*0,98*	48,03	48,26	3,70
K-29 E	γ	*-51%*	*-0,4*	*-0,1*	0,4	*-0,3*	0,4	*-0,5*	0,2	0,1	49	*0,99*	50,86	47,47	1,66
K-37 O	G-n	6%	0,3	0,6	0,7	0,9	0,9	0,1	*-3,2*	0,9	49	1,24	53,02	38,82	8,16
K-37 A	G-n	40%	0,3	0,6	0,7	0,9	0,9	0,0	*-3,7*	0,9	50	1,26	51,80	40,10	8,10
K-37 B1	G-n	33%	0,1	0,6	0,7	0,9	0,9	*-0,2*	*-4,0*	0,8	49	1,24	51,34	39,78	8,88
K-37 B2	G-n	23%	0,0	0,4	0,6	0,8	0,8	*-0,4*	*-4,4*	0,8	51	1,27	47,38	43,45	9,17
K-37 C	G-n	6%	*-0,2*	0,3	0,7	0,8	0,8	*-0,8*	*-6,0*	0,8	52	1,31	51,66	41,16	7,18
V4 E	β	*-65%*	*-1,7*	*-0,1*	0,9	0,8	1,0	*-1,3*	*-4,9*	0,8	52	1,34	66,07	30,71	3,22
V7 E	β	*-51%*	*-1,1*	*-0,3*	0,8	0,7	0,9	*-1,3*	*-5,3*	0,8	52	1,35	55,26	37,69	7,05
V7 B	β	*-50%*	*-1,1*	*-0,4*	0,5	0,7	0,8	*-1,4*	*-5,1*	0,6	53	1,38	49,09	35,88	15,03
V9 O	γ	*-1671%*	0,3	0,4	*-0,3*	*-1,0*	*-0,8*	0,6	*-0,5*	*-1,4*	32	*0,65*	25,83	54,88	19,29
V9 A	γ	15%	0,3	0,6	0,1	0,1	*-0,8*	0,7	0,7	0,4	37	*0,75*	38,45	37,11	24,44
V16 E	γ	*-102%*	*-1,4*	*-0,3*	0,6	0,2	0,5	*-0,8*	*-1,2*	0,7	51	1,02	59,71	36,35	3,94
V16 B	γ	*-191%*	*-2,4*	*-1,2*	*-0,2*	*-0,2*	*-0,3*	*-1,8*	*-2,2*	0,2	51	1,03	54,80	37,84	7,36
V15 O/A	P	*-123%*	*-0,8*	0,1	*-0,9*	*-0,6*	*-2,5*	0,5	0,5	*-2,6*	28	*0,73*	15,67	23,64	60,69
Rock samples															
Goletz Basalt											39		22,44	42,57	35,00
Gabbro-norite											40		22,88	51,73	25,39
TTG											50		43,63	49,91	6,46
Olivenite											40		13,48	6,15	80,37

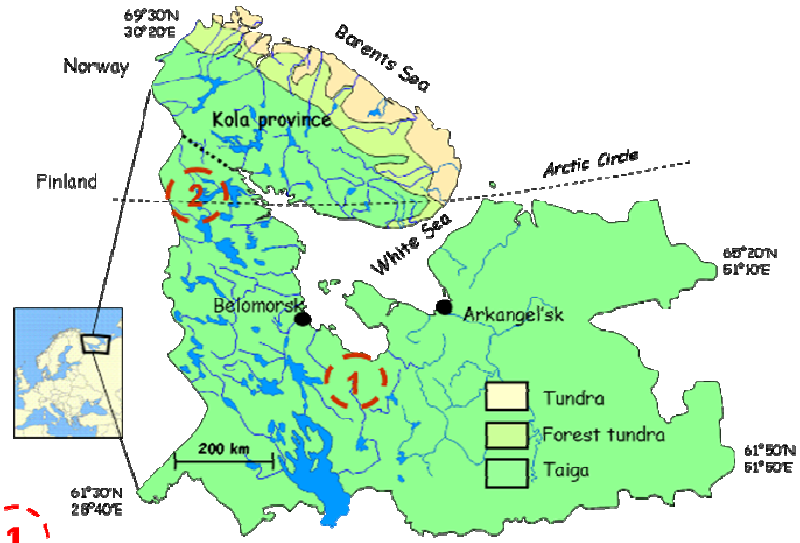

Fig. 1. Map of the studied areas Vetreny Belt paleorift (1) and Kivakka intrusion (2) showing soil (circles) and water (squares) sampling points and geological situation.

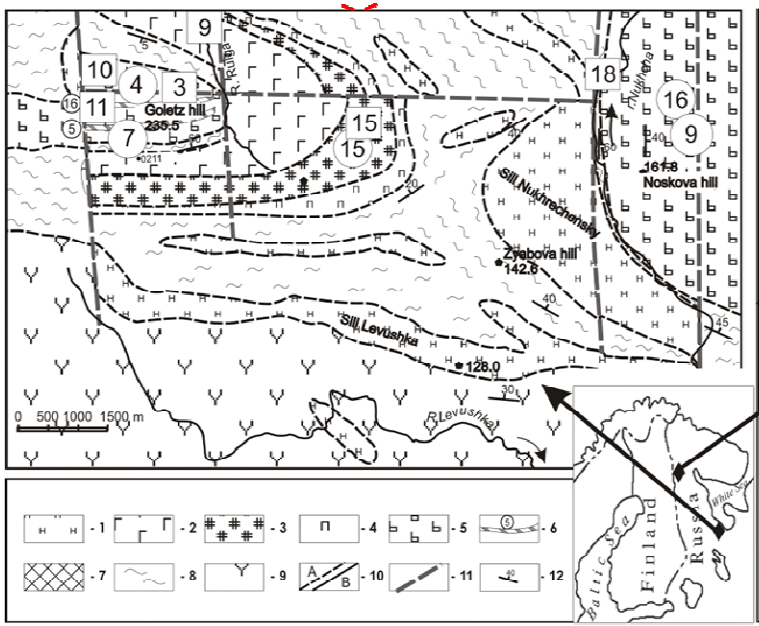

I. Schematic geological map of the Vetreny Belt (from Goletz hill to r. Nukhcha):
1 - nonsegmented mafit-ultramafit sils and dykes, *2* - gabbros, *3* - peridotites, *4* - pyroxenites, *5* - nonsegmented komatiitic basalts, *6* - differentiated covers 5 and 16 (in circles), *7* - probable supplying and deferent canals for prevolcanic camera Ruiga, *8* - Vileng suite sediments, *9* - Kirich suite vulcanites, *10* - geological borders (A - supposed, B - observed), *11* - faults, *12* - deposition elements.
Sample points and their numbers are marked with circles (soils) and squares (water).
Modified after Kulikov et al. (2008).

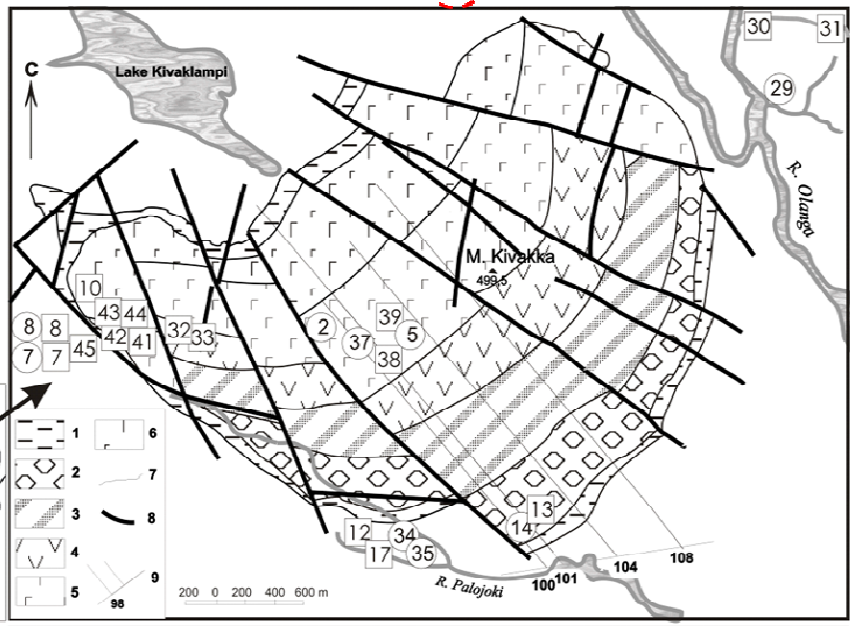

II. Schematic geological map of the Kivakka intrusion:
1 - Lower and Upper Contact Zones (LCZ and UCZ, respectively), *2* - Olivinite Zone (OZ), *3, 4* - Norite Zone (NZ), *3* - Subzone of Intercalating Bronzitites and Norites (SIBN), *5* - Gabbro--Norite Zone (GNZ), *6* - Zone of Gabbro-Norites with Pigeonite (ZGNp), *7* - geological borders, *8* - faults, *9* - profiles of YUKE PGO Sevzapgeologiya.
Sample points and their numbers are marked with circles (soil) and squares (water).
Modified after Bychkova and Koptev-Dvornikov (2004).

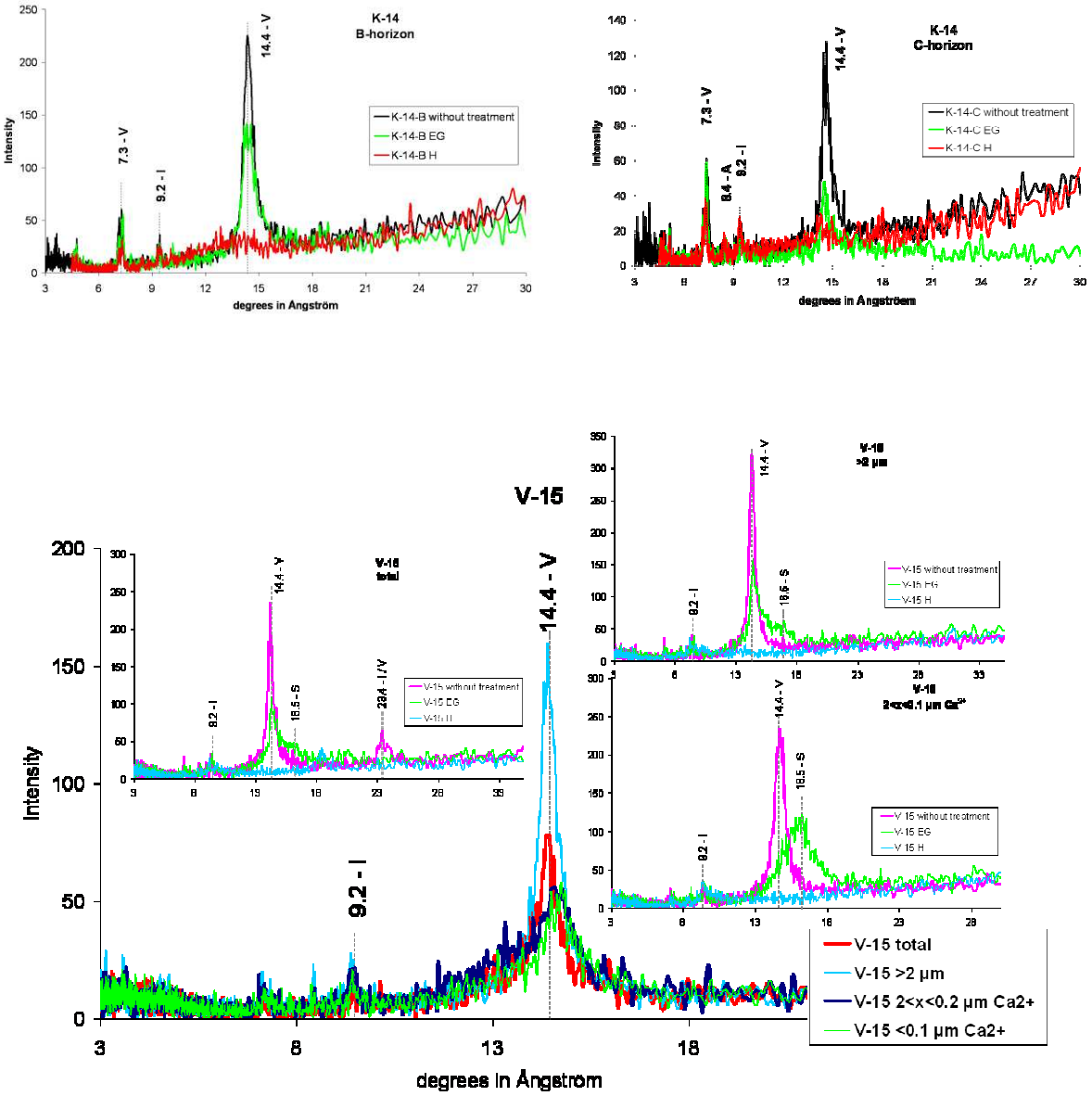

Fig. 2A. Representative X-ray diffractograms of soil profiles K-14 (upper panels) and V-15 (bottom panels). Minerals: I – illite, I/V – interstratified layers of illite and smectite, S – smectite, V – vermiculite. EG – ethylene-glycol saturation, H – heating, Ca^{2+} - calcium saturation.

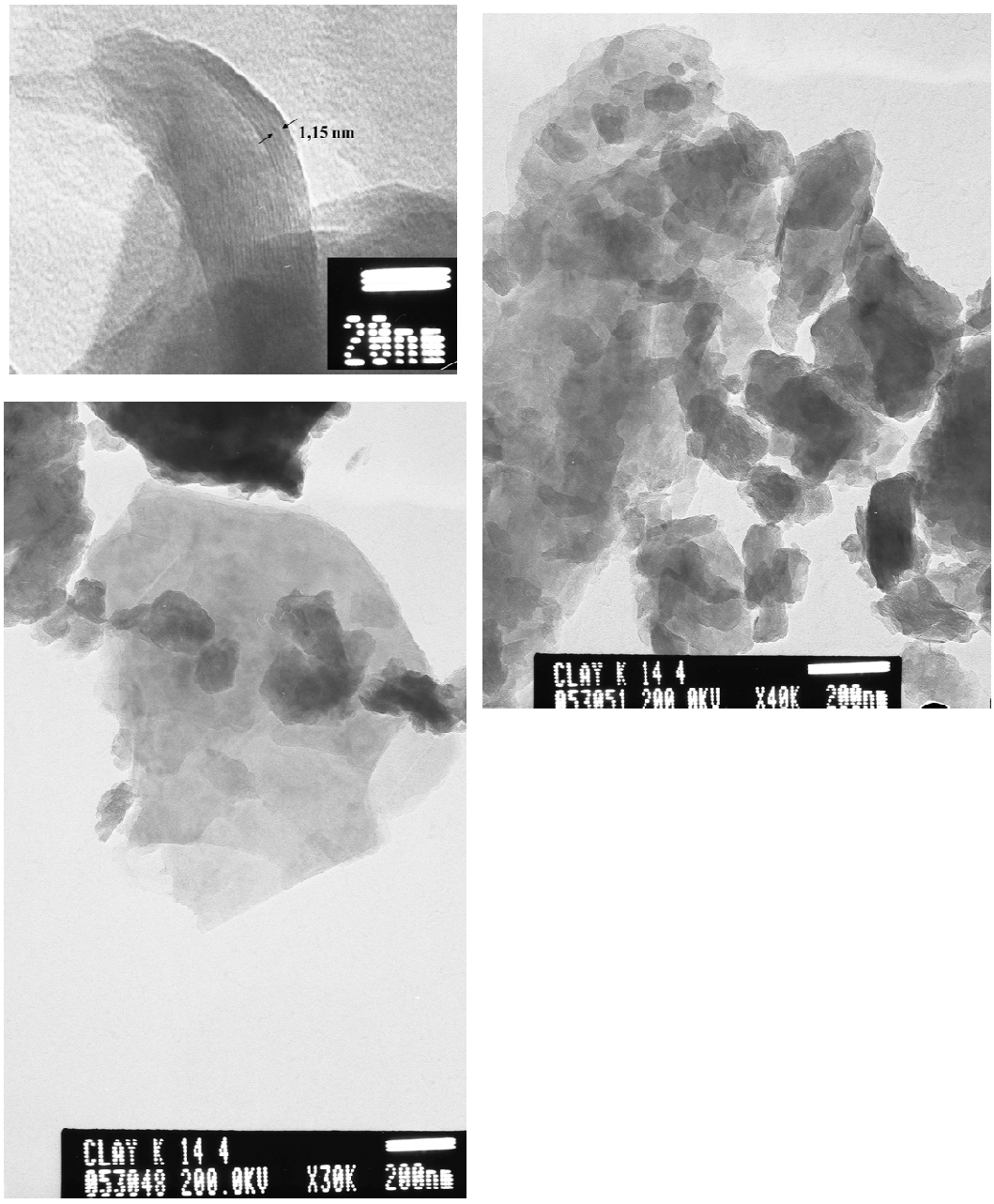

Fig. 2B. Transmission electron microscopy of clays in sample K-14.

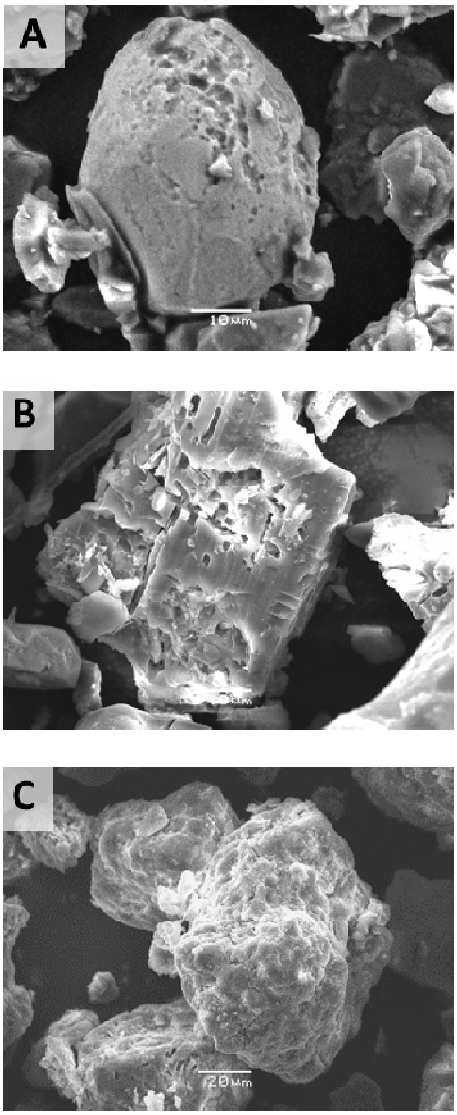

Fig. 3. SEM images of minerals found in soils illustrating neo-formed material and erosion on the surface of minerals: **A,** altered zircon in podzol V-16 over granite; **B,** altered feldspar in regosol K-29 over granite; **C,** quartz covered with aluminous coating in podzol K-37 over gabbro-norite.

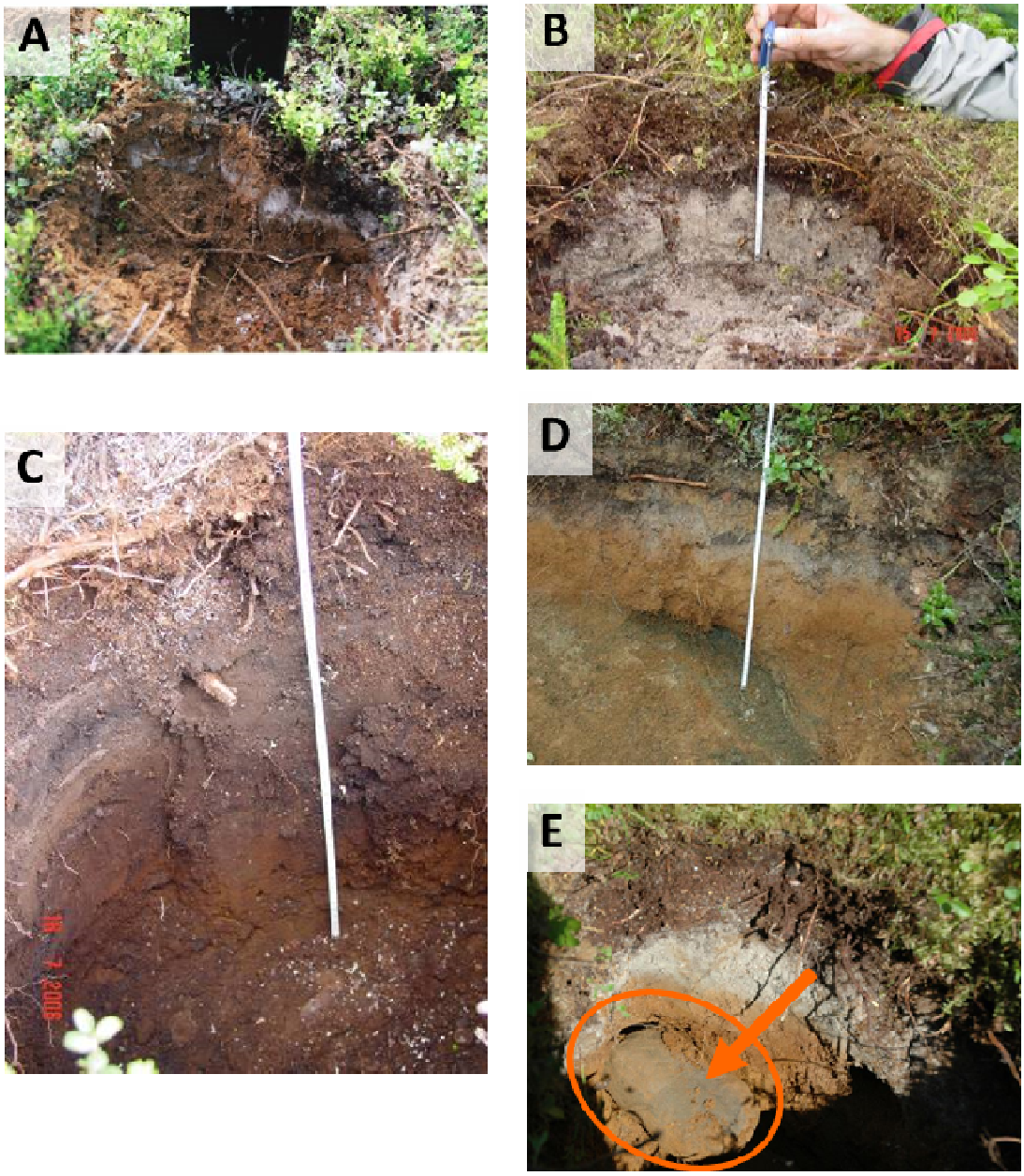

Fig. 4. Photos of podzol V-4 developed on komatiitic basalts from the Goletz hill of Vetreny Belt (A); the regosol K-29 under heather and bilberry bushes developed on gneiss from the Kivakka intrusion zone (B); the podzol K-37 developed on gabbro-norite rock of the Kivakka intrusion (C); the podzol K-14 developed on olivinite rock of the Kivakka intrusion (D) and podzol (K-7) developed on gneiss from the Kivakka intrusion zone (E). Full scale quaternary (Pleistocene) deposits can be observed in the deepest horizon confirming a strong moraine influence in this region.

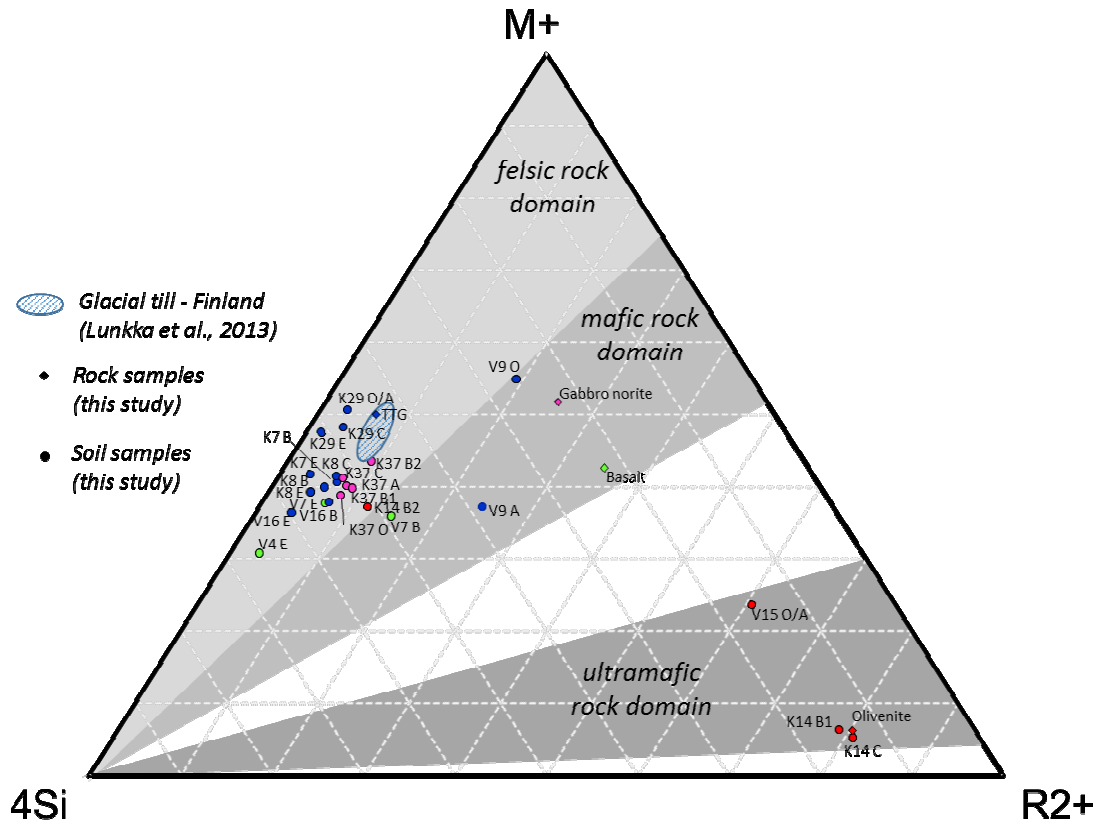

Fig. 5. WIS diagram including all the studied soil samples, Olivenite, Gabbro-norite, TTG rocks from Kivakka, Goltetz Basalt from Vetreny Belt and glacial till from Finland (Lunkka et al., 2013). See table 4 for calculations.

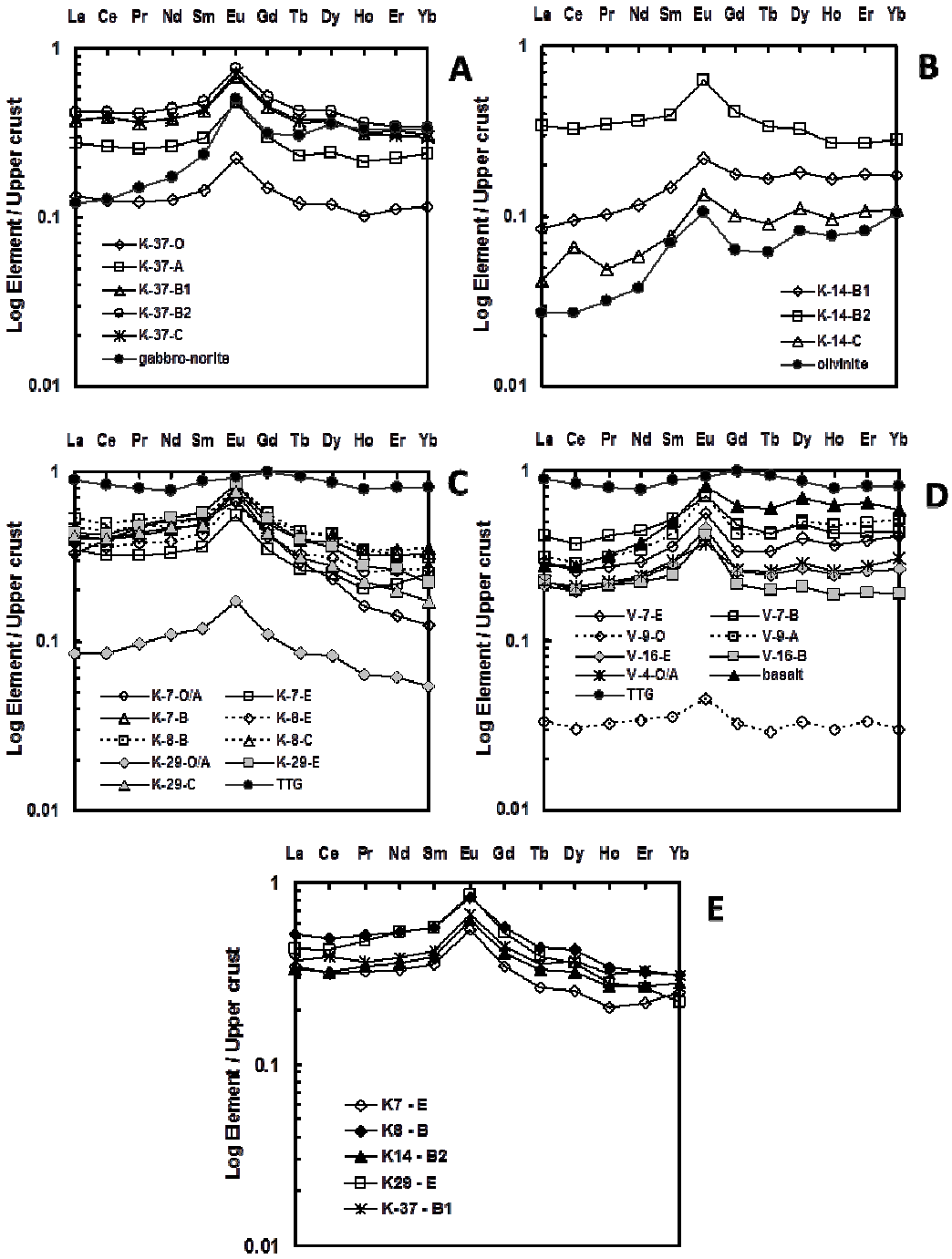

Fig. 6. Upper crust normalized REE patterns for soils from Kivakka intrusion (a, b, c), Vetreny Belt (d), and a mixed diagram on which E and B horizons of different soils are plotted (e). Average composition of the continental crust is taken from Taylor and MacLennan (1985); REE data on rocks of the Kivakka intrusion are from N. Krivolutskaya (unpublished data).

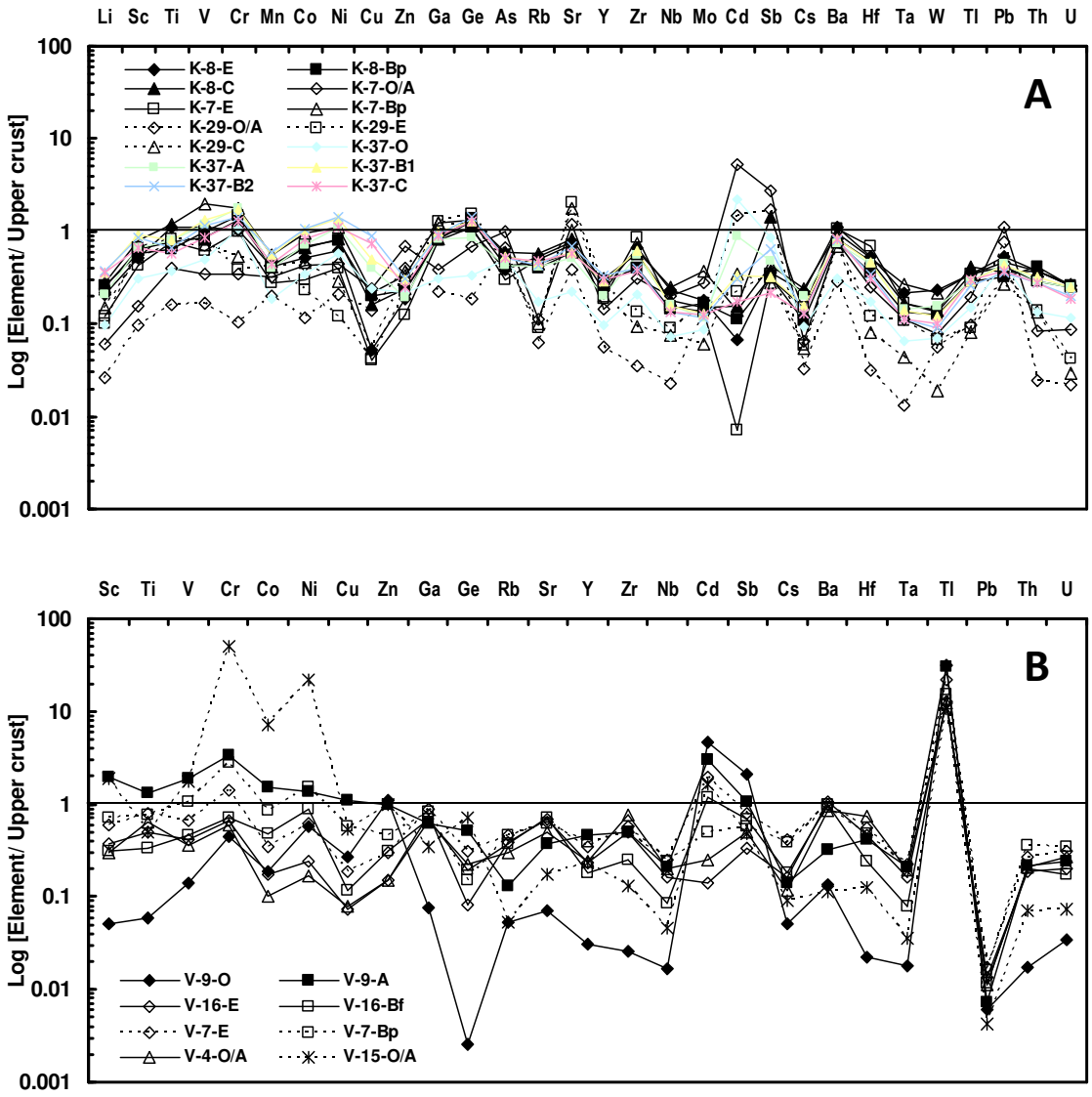

Fig. 7. Upper crust (Taylor and MacLennan, 1985) normalized extended elements patterns for soils developed on both felsic and mafic rocks from the Kivakka intrusion zone (A) and Vetreny Belt zone (B).

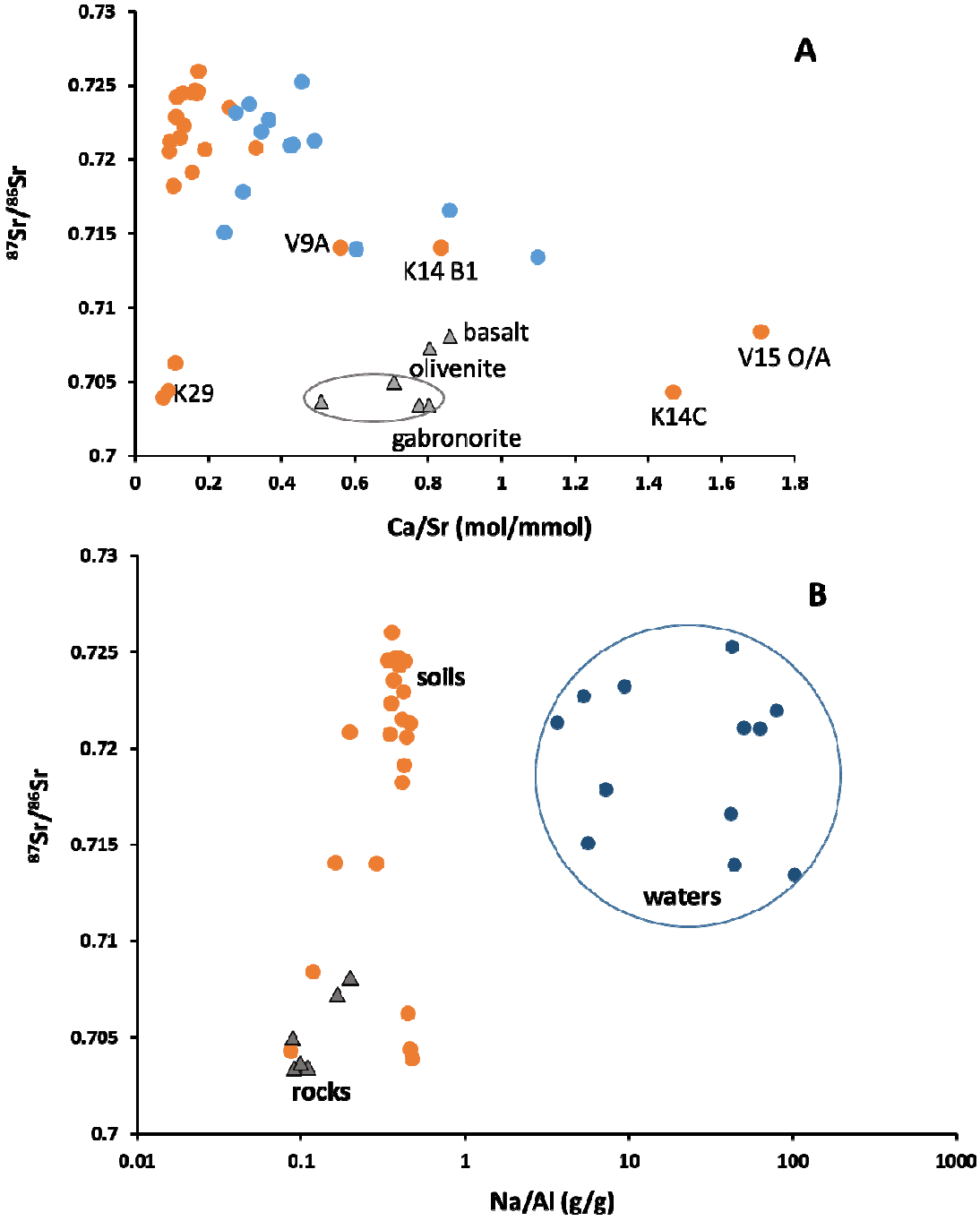

Fig. 8. Sr isotope ratio versus Ca/Sr ratio of soils and rocks (A) and Sr isotope ratio in soils, rocks and waters versus Na/Al ratio as indicator of weathering degree.

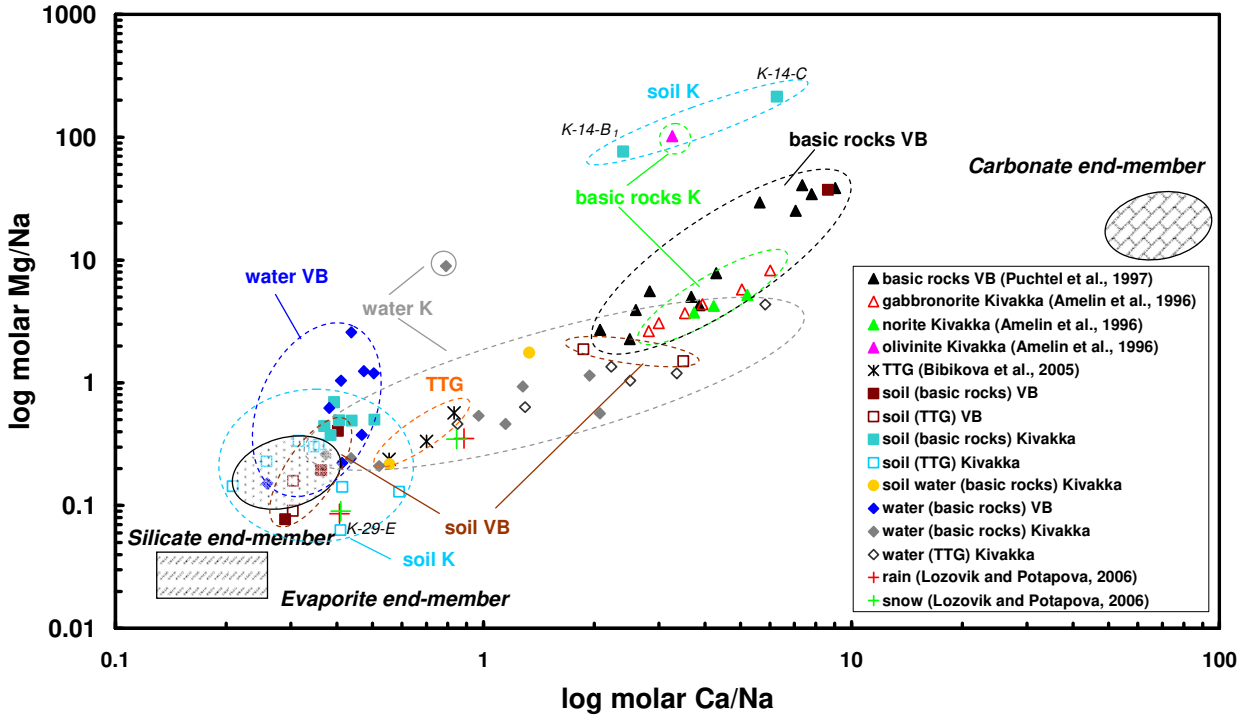

Fig. 9. Ca/Na molar ratios vs. Mg/Na molar ratios showing different materials (soils, rocks and waters) from Kivakka intrusion and Vetreny Belt (VB) zones. The carbonate, silicate, and evaporate end-members are taken from Gaillardet et al. (1999). Atmospheric signatures are calculated from the data reported by Lozovik and Potapova (2006). "VB" and "K" on the diagram stand for Vetreny Belt and Kivakka intrusion zones, respectively. Note that the scale of X and Y axes is different.

Chemical weathering of mafic rocks under granitic moraine in the subarctic